ASSESSING DRIVEN STEEL PILE CAPACITY ON ROCK USING EMPIRICAL APPROACHES

by

Timothy Morton

Submitted in partial fulfilment of the requirements
for the degree of Master of Applied Science

at

Dalhousie University
Halifax, Nova Scotia
August 2012

DALHOUSIE UNIVERSITY

DEPARTMENT OF CIVIL AND RESOURCE ENGINEERING

The undersigned hereby certify that they have read and recommend to the Faculty of Graduate Studies for acceptance a thesis entitled "Assessing Driven Steel Pile Capacity on Rock Using Empirical Approaches" by Timothy Morton in partial fulfilment of the requirements for the degree of Master of Applied Science.

Dated: August 17th, 2012

Supervisor: ____________________________

Dr. Craig Lake

Readers: ____________________________

Dr. Don Jones

____

Joseph Moore

DALHOUSIE UNIVERSITY

DATE: August 17th, 2012

AUTHOR: Timothy Morton

TITLE: Assessing Driven Steel Pile Capacity on Rock Using Empirical Approaches

DEPARTMENT OR SCHOOL: Department of Civil and Resource Engineering

DEGREE: MASc CONVOCATION: October YEAR: 2012

Signature of Author

TABLE OF CONTENTS

LIST OF TABLES

LIST OF FIGURES

ABSTRACT

Small displacement driven steel piles are a very advantageous deep foundation system when encountering rock because of the durable nature of steel and their ability to penetrate dense materials during the driving process. However, methods of estimating the ultimate toe resistance of these piles in this condition are scarce in design codes. This thesis attempts to address this lack of guidance by inspecting various design techniques of determining ultimate toe capacity of these types of piles and comparing them to field measured values.

Methods of determining pile toe capacity for both small displacement driven steel piles and drilled sockets were collected. Working in conjunction with a local consulting firm, records of previous pile driving sites were collected. A process to determine quality data for use in this work was developed by the author including information from geotechnical site investigations, pile driving records and pile driving analysis (PDA) records.

By plotting unconfined compressive strength of rock versus measured ultimate pile toe capacity of these piles, a best fit line of $7.5q_u$ and a series of confidence intervals were established for the site records. This best fit line was compared to all of the previously reviews design methods for calculating ultimate pile toe capacity. It was found that most of the methods for drilled sockets were overly conservative when applied to small displacement driven steel piles; this was expected as the presence of rock discontinuities tends to have a stronger effect on drilled caissons. An author reinterpretation of the method developed by Ladanyi and Roy (1971), justified by the difference in influence in rock discontinuity on pile toe capacity, showed good agreement with the measured field data. The most effective existing method was determined to be that of Rehnman and Broms (1971), as it was the only method developed for small displacement driven steel piles.

Data points not previously used in the filtering process (because of lack of rock strength testing) was then used in an attempt to verify the best fit of the data previously developed by the author. Ranges of rock strength estimated from the rock descriptions were used in this process. It was found that the best fit and confidence limits developed by the author adequately predicted the pile toe capacity, at least from a design perspective. A pile case from Masumoto (1995) was also investigated, but it provided less promising results, likely due to the very low rock strength of the case.

LIST OF ABBREVIATIONS AND SYMBOLS USED

LIST OF ABBREVIATIONS

BOR	Beginning of re-strike
CAPWAP	Case Pile Wave Analysis Program
CFEM	Canadian Foundation Engineering Manual
EOID	End of initial drive
FHWA	Federal Highway Administration
PDA	Pile Driving Analyzer
PDA-W	Pile Driving Analyzer program
RQD	Rock Quality Designation
WEAP	Wave Equation Analysis of Piles

LIST OF SYMBOLS

A = cross sectional area of pile (L^2)

A_s = side friction area (L^2)

A_t = toe bearing area (L^2)

a = net area ratio (for cone penetrometer test)

B = pile base diameter (mm)

B_s = diameter of socket (L)

C = spacing of discontinuities (L)

c = cohesion (F/L^2)

c_u = undrained shear stress (F/L^2)

c_v = wave propagation velocity (speed of sound in pile) (L/t)

D = depth of foundation (L)

d = CFEM (2006) depth factor

d_c = Ladanyi and Roy (1971) depth factor

d_{Mc} = Meyerhof (1963) depth factor

E = elastic modulus of pile (P/L^2)

F = force in pile (F)

f_s = ultimate unit side friction resistance (F/L^2)

K_p = active earth pressure

K_{sp} = an empirical coefficient, based on rock discontinuity aperture and spacing and pile diameter

L = length of pile (L)

L_s = depth (length of socket) (L)

l = foundation length (L)

m = factor based on rock properties

N_c = bearing capacity factor

N_k = cone bearing factor

N_q = bearing capacity factor

N_γ = bearing capacity factor

N_ϕ = bearing capacity factor

P = pile load (F)

P_u = ultimate pile capacity (F)

p = overburden pressure (F/L^2)

q = ultimate bearing capacity (F/L^2)

q_c = cone tip resistance (F/L^2)

q_t = ultimate toe bearing resistance (F/L^2)

q_{tc} = ultimate calculated toe bearing resistance (F/L^2)

q_{TC} = corrected cone tip resistance (F/L^2)

q_u = average unconfined compressive strength of rock (F/L^2)

RQD = Rock quality designation (%)

s = factor based on rock properties

T_f = shear stress on the plane of failure (F/L^2)

T_s = uniaxial tensile stress (F/L^2)

t = time

u = displacement of the pile at depth z (L)

u_{bt} = pore water pressure behind piezometer tip (F/L^2)

v = particle velocity in pile (L/t)

W = width of foundation (L)

W_p = weight of pile (F)

x = horizontal offset movement from initial elastic portion of load deflection curve (mm)

Z = pile impedance (F*t/L)

z = depth below ground surface (L)

α = best fit constant of q_t vs. q_u plot

β = shaft resistance empirical parameter

γ = unit weight of soil (F/L^3)

η = best fit factor

Δ = movement of pile base (L)

Δ_u = ultimate pile base movement (L)

δ = aperture of discontinuities (L)

ϕ = friction angle (degrees)

λ = average number of discontinuities per meter (L^{-1})

ν = best fit factor

ρ = density of pile material (M/L^3)

σ = normal stress on failure plane (F/L^2)

σ_{vo} = overburden stress (F/L^2)

σ_1 = major principal stress (F/L^2)

σ_3 = minor principal stress (F/L^2)

τ = shear stress (F/L^2)

ACKNOWLEDGEMENTS

First I would like to express my gratitude to my supervisor Dr. Craig Lake for his guidance not only throughout the length of this process, but also in my initial decision to pursue graduate studies. Without his expertise and patience, this project certainly would not have come to fruition.

I would like to thank Joseph Moore, for his input and support of this project and for supplying his knowledge of the subject matter. I would also like to thank both him and Dr. Don Jones for serving on my committee.

I would like to thank the Natural Sciences and Engineering Research Council of Canada (NSERC) and the Dartmouth office of Stantec Consultants Inc. for funding this work and financially making this research possible. I would like to thank the employees of Stantec, especially Greg MacNeill and Todd Menzies, for their continuing supply of knowledge in the subject matter and Peter Crowe and Brian Grace, for their interest and aid in the project. Both Marleigh Leaman of Stantec and Jesse Keane of Dalhousie assisted greatly with various laboratory testing for this project as well.

Lastly I would like to express my appreciation to my family and my closest friends for their encouragement and support throughout my graduate studies.

CHAPTER 1 INTRODUCTION

1.1 General

Deep foundations become necessary for construction sites where the near surface soils provide inadequate support for the structural loads present. They may also be required for structures adjacent to bodies of water that can cause scouring or undermining of foundations or for cases where uplift resistance is required from the foundation (Coduto, 2001).

Although there are many various forms of deep foundations, the resistances afforded by these foundations are usually developed from the side frictional resistance and toe resistance. Shaft friction is developed from the association of the soil or rock along the length of the pile; meanwhile toe resistance is developed from the soil shear capacity at the toe of the pile structure. Mathematically, this ultimate resistance capacity, P_u, can be expressed as (Coduto, 2001):

[1] $$P_u = \Sigma f_s A_s + q_t A_t - W_p$$

Where:

P_u = ultimate pile capacity (F)

f_s = ultimate unit side friction resistance (F/L^2)

A_s = side friction area (L^2)

q_t = ultimate toe bearing resistance (F/L^2)

A_t = toe bearing area (L^2)

W_p = weight of pile (F)

Using steel driven piles for deep foundation design has a number of benefits. In the Halifax area, much of the soil conditions consist of different varieties of glacial tills. These tills contain a high percentage of gravel and also contain frequent boulders (Lewis et. al., 1998). In many parts of Canada, glacial till is quite common as well (Legget, 1976). Coduto (2001) explains that concrete piles are not capable of being driven where difficult driving conditions are present, while augering is difficult where cobbles or boulders are present. Steel piles, especially H-piles and open ended pipe piles, are characterized as small displacement piles. The small displacement of soil during driving allows gravel and cobbles to be displaced and hence make the use of these small displacement durable steel piles desirable.

Coduto (2001) also explains that since steel is much stronger in tension than any concrete substitute, steel piles are essential for any design requiring large tensile loads. Steel piles are also very easy to cut and to splice through welding or special steel splicers, making it very easy to change the pile lengths required for sites with changing geological conditions. The three major rock formations in the Halifax region, which also extend to cover a major portion of peninsular Nova Scotia, are characterized by sloping caused by erosion by rivers and glaciers (Lewis et. al., 1998). This has a profound effect on the deep foundation method selected as uneven bedrock and potential shallow rock formations will likely be encountered. These again are conditions that favor the usage of steel piles (Coduto, 2001).

One issue associated with the usage of small displacement steel piles driven to rock is that there are few empirical or theoretical design methodologies available. This can likely be attributed to difficulties in determining precise in-situ rock details and the complexities of pile and rock interactions. This has led to driven small displacement steel piles into rock being largely ignored in multiple design codes. The American Federal Highway Administration (FHWA, 1998) simply states that "determination of load capacity driven piles on rock should be made on basis of driving observations, local experience and load". For design purposes, empirical methods are used for estimation of steel driven pile capacities, but not without extensive field testing to ensure that these capacities are met.

1.2 Research Objectives

As mentioned in the previous section, the toe capacity of driven small displacement steel piles is not a major focal point of design codes. The overall purpose of this thesis is to review all known methods of estimating toe capacity of low displacement driven steel piles in order to recommend the most appropriate and accurate method of estimating this ultimate pile toe capacity. It is hypothesized that through the knowledge of geotechnical site information, including rock strength, pile depth and "complete" pile details, that the toe capacity can be adequately predicted with some level of reliability.

To achieve these goals and investigate the hypothesis, this thesis was organized into a series of chapters. Chapter 2, entitled "Literature Review", reviews all existing theories and methods associated with driven pile capacity. A collection of empirical and theoretical approaches of estimating capacity of drilled pile capacities, that may or may not be appropriate for driven steel piles, is also reviewed. The process of measuring pile resistance in the field is also outlined in Chapter 2 as it is important to understand the field process used to obtain the majority of the data in this research (i.e. Pile Driving Analyzer). Chapter 3, entitled "Data Collection", reviews the developed progression of acquiring, screening and compiling previous site data in order to analyze these methods. Chapter 3 outlines the developed data collection process in its entirety. It lists the documentation required to proceed with the gathering of data and also describes the parameters that are considered essential to complete a data set. Lastly, Chapter 3 presents the data to be examined throughout this thesis. Chapter 4, entitled "Results and Discussions", compares the data set developed from the screening process and compares it to the empirical and theoretical relationships presented in Chapter 2 for toe capacity estimation in rock. Lastly, Chapter 5, entitled "Comparing Empirical Relationships to Other Data Sources", uses data excluded from the database created in Chapter 3 and data from literature in an attempt to verify the best fit method developed in Chapter 4.

CHAPTER 2 LITERATURE REVIEW

2.1 Ultimate Bearing Resistance Of Piles In Rock: Available Theories

Unlike soil, rock is typically brittle and its failure in shear is a function of both the rock properties and the discontinuities that exist in the rock mass. Brittle materials are very complex; they depend heavily on a system of micro-cracks throughout the material and thus there exists no mathematical formula for this behavior (Pells and Turner, 1978). For this reason, many rock failure theories assume rock to have a plastic failure because its peak failure envelope is often curved (Pells and Turner, 1978). When assumed to be plastic, rock follows the Mohr-Coulomb failure criterion (Pells and Turner, 1978). The Mohr-Coulomb rupture failure criterion can be seen as follows (Meyerhof, 1951):

[2] $$\tau = c + \sigma \tan \phi$$

Where:
τ = shear stress (F/L^2)
c = cohesion (F/L^2)
σ = normal stress on failure plane (F/L^2)
ϕ = friction angle (degrees)

Another strength failure theory is that developed by Griffith, as discussed in Coates (1981). This theory is based on fracture mechanics, and deals with mechanics of all material properties. For rock structures, Griffith's Failure Theory is based on the presence of microscopic cracks in a rock material, of which concentrations of stress can exist. When loaded, these cracks can propagate, inducing material failure. Griffith's failure theory can be described as follows in equation 3, as seen in Coates (1981):

[3] $$T_f = 2\sqrt{T_s\sigma + T_s^{\,2}}$$

Where:

T_s = uniaxial tensile strength (F/L^2)

T_f = shear stress on the plane of failure (F/L^2)

Terzaghi (1943) used the Mohr-Coulomb failure criterion to describe the ultimate bearing capacity of a strip footing foundation, which can be seen as follows:

[4] $$q = cN_c + pN_q + \gamma\frac{W}{2}N_\gamma$$

Where:

q = ultimate bearing capacity (F/L^2)

p = overburden pressure (F/L^2)

γ = unit weight of soil (F/L^3)

W = width of foundation (L)

N_c = bearing capacity factor

N_q = bearing capacity factor

N_γ = bearing capacity factor

Pells and Turner (1978) explain that cohesion has vastly superior effects on the Terzaghi (1943) equation for rock materials. Since the cohesion element is considered much larger than the other parts of this equation, the other parts can be considered negligible and this formula can be condensed into (Pells and Turner, 1978):

[5] $$q = c\frac{N_c}{2\sqrt{N_\phi}}$$

Where:

[6] $$N_\phi = \tan^2\left(45 + {}^{\phi}/_{2}\right)$$

N_ϕ = bearing capacity factor

Meyerhof (1963) explains that that the bearing capacity for a circular or square foundation can be found by multiplying the bearing capacity of a strip footing by a set of modification factors. For the cohesion portion of the equation 4, the factor is as follows (Meyerhof, 1963):

[7] $$s_c = 1 + 0.2N_\phi\,{}^{W}/_{l}$$

Where:

s_c = circular bearing capacity factor

l = foundation length (L)

Meyerhoff (1963) also explains that the bearing capacity of a foundation also can be affected by the shearing resistance of the soil above the foundation level. Again, this can be taken into account by multiplying equation 4 by a series of factors. The factor for the cohesion portion of the Terzaghi (1943) formula is as follows:

[8] $$d_{Mc} = 1 + 0.2\frac{D}{W}\sqrt{N_\phi}$$

Where:

d_{Mc} = Meyerhof (1963) depth factor

D = depth of foundation (L)

2.1.1 Bell (1915) Solution

In 1915, Bell devised a method to approximate ultimate bearing capacity based on the unconfined compressive strength of rock. This method examines a foundation placed on a smooth surface. It assumes that the rock below the foundation is in a Rankine active state and that the rock immediately surrounding this area is in a Rankine passive state (Pells and Turner, 1978). When there is no surcharge above the passive zone, this leads to a stress state equation of (Pells and Turner, 1978):

[9]
$$\sigma_1 = \sigma_3 N_\phi + 2c\sqrt{N_\phi}$$

Where:

σ_1 = major principal stress (F/L^2)

σ_3 = minor principal stress (F/L^2)

For most footings on rock, the minor principal stress, which in this case represents the body force due to gravity, can be represented by equation 10 (Pells and Turner, 1978).

[10]
$$\sigma_3 = 2cN_\phi$$

When considering equation 10 with the Mohr-Coulomb failure theory, this leads to an approximate bearing capacity in the active zone as described by Bell (1915) as seen in equation 11 (Pells and Turner, 1978).

[11]
$$q = q_u\left(N_\phi + 1\right)$$

Where:

q_u = average unconfined compressive strength of rock (F/L^2)

2.1.2 Coates (1981)

Coates (1981) performed a similar analysis to Bell (1915), except that it was assumed that the rock conforms to the Griffith's Failure Theory. Pells and Turner (1978) explain that for this method, equation 9 becomes:

[12] $$\sigma_1 = q_u$$

Through looking at wedge analysis, an equation for ultimate bearing capacity can be produced as shown in equation 13 by substituting equation 12 into Griffith's Failure theory (Pells and Turner, 1978).

[13] $$q = 3q_u$$

2.2 Semi- Empirical Equations To Predict Toe Capacity of Small Displacement, Steel Piles Driven to Rock

2.2.1 Rehnman and Broms (1971)

Rehnman and Broms (1971) developed a method to estimate the tip resistance of a steel pile driven into rock, directly based on the rock's unconfined compressive strength. Rock samples of granite, limestone and sandstone were encased in steel cylinders and surrounded by cured concrete prior to coring via an air hammer. The holes were filled with a rod of the same diameter. The air hammer was used to simulate the pile driving process. After compiling the laboratory results and unsuccessfully comparing results to both Mohr-Coulomb and Griffith failure criteria, Rehnman and Broms (1971) compared the ratio of ultimate toe bearing resistance (q_t) to average unconfined strength of the rock (q_u) tested. From the experimental data, it was found that the average ratio of q_t/q_u was 6.2 for granite, 5.2 for limestone and 4.8 for sandstone (Rehnman and Broms, 1971). After comparing the results with different failure theories, Rehnman and Broms (1971) found that the results for the most brittle rocks (i.e. limestone and granite) most resembled that of the Griffith's Failure Theory (Rehnman and Broms, 1971) but under-predicted capacities by 50%. The more ductile sandstone was better predicted with Mohr-Coulomb. Rehnman and Broms (1971) went further and suggested that the ultimate toe capacity of driven piles on flat rock surfaces with minimal embedment could be predicted empirically using equation 14:

$$q_t = 4 \text{ to } 6q_u \tag{14}$$

This range of 4 to 6 was based on the experimental results of 4.8 to 6.2 and takes into consideration the range of rock strengths. Through work in the Atlantic provinces, local practice suggests that q_t be limited to 225MPa, which essentially related to the strength of steel (MacNeill, personal communication, 2010).

2.3 Equations For Predicting Toe Capacity of Socketed Concrete Piles Drilled into Rock

2.3.1 Ladanyi and Roy (1971)

Ladanyi and Roy (1971) introduced a method for evaluating the toe capacity of drilled piles, developed through the use of plasticity theory. The method takes into consideration both the nature of the rock and the depth of embedment of the pile in this rock. Although not intended for use with driven steel piles, the lack of design methodologies of piles driven into rock often results in its use in Canada (MacNeill, personal communication, 2010).

This original equation presented by Ladanyi and Roy (1971) is shown in equation 15. The equation attempts to theoretically describe experimental lab testing the authors (i.e. Ladanyi and Roy, 1971) were producing. This work included a series of penetration tests in a solid rock sample with varying embedment depths. From their testing, they found that a bulb of crushed rock formed immediately below the cylindrical load. However, when the cylindrical load was embedded in the rock, radial cracking surrounded this bulb. This method combines the work of Bell (1915) as seen in equation 11 and the depth factor developed by Meyerhof (1963) as seen in equation 8.

[15] $$q_t = q_u(K_p + 1)d_c$$

Where:

K_p = active earth pressure

d_c = Ladanyi and Roy (1971) depth factor

The depth factor used by Ladanyi and Roy (1971) differs slightly from that of Meyerhof (1963) and can be seen in equation 16.

[16] $$d_c = 1 + 0.5\frac{L_s}{B_s}\cos\phi$$

where:

L_s = depth (length of socket) (L)

B_s = diameter of socket (L)

The original form of Ladanyi and Roy (1971) depended highly on the friction angle of rock. The passive earth pressure depends only on the friction angle of rock, while the depth factor is also very dependent on this parameter. More recent literature presents the work of Ladanyi and Roy (1971) much differently. Equation 17, as listed in the Canadian Foundation Engineering Manual (CFEM , 2006) is as follows:

[17] $$q_t = (FS)q_u K_{sp} d$$

Where:

[18] $$d = 1 + 0.4\frac{L_s}{B_s} \text{ where } d \leq 3$$

K_{sp} = an empirical coefficient, based on rock discontinuity aperture and spacing and pile diameter

d = CFEM (2006) depth factor

FS = factor of safety

This equation typically requires a factor of safety of 3, but this factor of safety can range as high as 10 (CFEM, 2006). The K_{sp} variable relates to a relationship between spacing and aperture of rock discontinuities with respect to footing width rather than using a passive earth pressure constant dependent on friction angle. Table 1 below provides estimated values of K_{sp} based on a discontinuity spacing description (CFEM, 2006).

Table 1 Coefficients of discontinuity spacing (CFEM, 2006)

Discontinuity Spacing		
Description	**Distance (m)**	**K_{sp}**
Moderately Close	0.3 to 1	0.1
Wide	1 to 3	0.25
Very Wide	>3	0.4

Equation 19 and Figure 1 below (CFEM, 2006) can be used to calculate K_{sp} if sufficient information is known.

[19]

$$K_{sp} = \frac{3 + {}^{C}/_{B_s}}{10\sqrt{1 + 300\,{}^{\delta}/_{C}}}$$

Where:

C = spacing of discontinuities (L)

δ = aperture of discontinuities (L)

valid for: $0.05 < C/B_s < 2.0$ and $0 < \delta/C < 0.02$

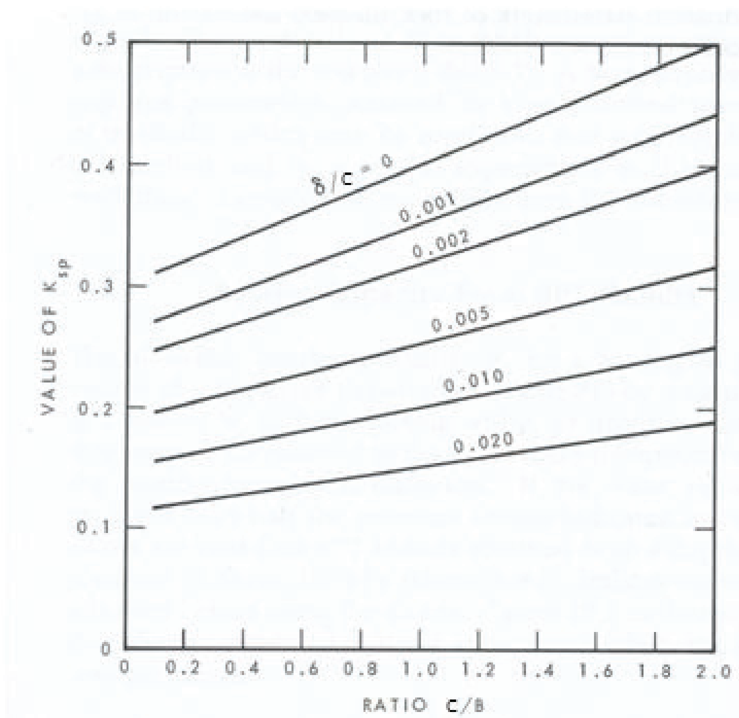

Figure 1 K_{sp} values for typical aperture widths and discontinuity spacing (CFEM, 2006)

Ladanyi and Roy (1971) state that the depth factor equation "predicts a linear increase of lower bound resistance with the depth of embedment, but is obviously acceptable only at shallow depths, not exceeding 5 or 6 diameters of the punch." A further examination of this "5 or 6 diameters of the punch" with the original depth factor of "d_c" is shown below in Figure 2. This graph shows that for ranges of common friction values for rock, varying factors of L/B ranging from 0 to 5 produce values of "d_c" of a minimum of 1 to a maximum of around 3. It is likely this practicality of limited "d_c" was introduced into the design approach later in the CFEM (2006).

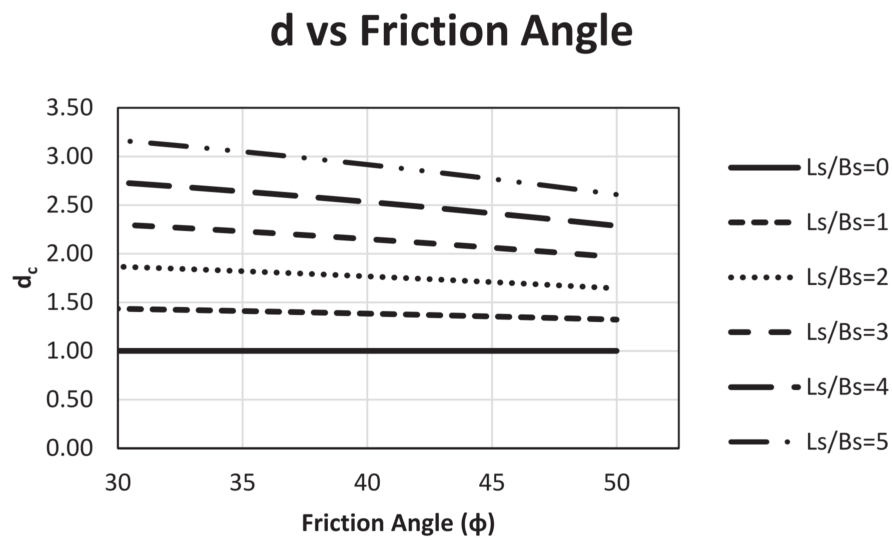

Figure 2 Values of d_c with respect to friction angle

A practical problem with equation 19 is that aperture and spacing are not frequently measured in typical geotechnical investigations. These measurements can be very tedious and would require measurements in a very specific area of the site (i.e. exactly where foundation tip would be loaded). One method to estimate the value of K_{sp} for typical geotechnical projects is through the use of the commonly measured RQD (rock quality designation) which was developed by Deere (1963) for tunneling through rock. The RQD parameter has since been adapted for rock classification purposes. For RQD to be properly defined, a core length of at least 100 mm must be retrieved. Deere and Deere (1988) define RQD as a means of describing the percentage of sound rock in a given borehole, which is calculated by:

[20]
$$\mathrm{RQD}(\%) = \frac{\sum \text{Lengths of core pieces} > 10cm}{\text{Total core length}} \text{ X } 100$$

where:

RQD = Rock quality designation (%)

Since RQD includes no measurement in aperture or spacing of rock joints, there is no direct relationship between RQD and these parameters. A study by Priest and Hudson (1976) developed a method in order to statistically estimate mean discontinuity spacing of rock joints through RQD measurements using a negative exponential distribution of data. It was found that when the average number of discontinuities per meter was between 6 and 16, equation 21 could be used to estimate the average number of discontinuities, λ . When "λ" is not between 6 and 16, using equation 22 with trial and error was proven to be more reasonable.

[21] $$\lambda = 30 - \frac{\mathrm{RQD}}{3.68} \quad [6 < \lambda < 16]$$

[22] $$\mathrm{RQD} = 100e^{-0.1\lambda}(0.1\lambda + 1) \quad [\lambda < 6 \; or \; \lambda > 16]$$

where:

λ = average number of discontinuities per meter (L^{-1})

To calculate the average discontinuity spacing, the inverse of this "λ" value can be taken to produce the discontinuity spacing in meters.

2.3.2 Rowe and Armitage (1987)

Rowe and Armitage (1987) developed an empirical relationship similar to Coates (1981) and Rehnman and Broms (1971). This equation is empirically based on the static load testing (to be discussed later) results of 12 socketed piles in soft rock from three separate papers and can be seen below:

[23] $$q_t = 2.5q_u$$

Rowe and Armitage (1987) reference Hovarth et. al. (1983) who presented static load testing results for a mudstone with an unconfined compressive strengths ranging from 4.7 to 11.1 MPa. The two load tests recorded from this article had yet to exceed the elastic region of the load-displacement curve and hence the ultimate socket resistance was not reached; the two load tests were terminated at $0.96q_u$ and $1.35q_u$. Another article referenced in Rowe and Armitage (1987) is that of Glos et. al. (1983). This article looked at two load tests on soft shaley sandstones with unconfined compressive strengths of 8.4 MPa and 9.3 MPa. These tests contained load displacement curves that had moved into the plastic zone, but finished with the curve still rising steeply; terminating at $0.95q_u$ and $1.25q_u$ respectively. The third article referenced is that by Williams (1980) contained 8 pile load test results demonstrated piles yielding at $1.4q_u$ to $2.5q_u$, with pile load testing ending between $2.5q_u$ and 10.5 q_u. Overall, it can be seen that this method may be a good conservative relationship to use in design of socketed piles.

2.3.3 Zhang and Einstein (1998)

Zhang and Einstein (1998) developed an empirical method similar to that completed by Rowe and Armitage (1987) for drilled sockets into rock. They compiled a collection of 39 pile load tests found in the literature, including two of the three sources used in Rowe and Armitage (1987) but excluding Hovarth et. al. (1983). The majority of these cases were for sockets on weak rocks. Zhang and Einstein (1998) plotted the best fit line through these data points to produce the following equation:

[24] $$q_t = 4.83(q_u)^{0.51}$$

The value of 4.83 in this equation is an average value, with a conservative upper bound solution of 6.6 and a lower bound solution of 3.0.

2.3.4 Hoek and Brown (1980)

Another method for designing for toe resistance of drilled sockets in a jointed rock formation has been developed by Hoek and Brown (1980). They used their theoretical and experimental experiences to develop an empirical relationship as follows:

[25] $$\sigma_1 = \sigma_3 + \sqrt{m q_u \sigma_3 + s {q_u}^2}$$

Where:

m = factor based on rock properties (see discussion below)

s = factor based on rock properties (see discussion below)

Hoek and Brown (1980) explain that "m" and "s" are empirically defined constants based on rock properties. Carter and Kulhawy (1988) describe these factors as analogous with "c" and "ϕ" in the Mohr-Coulomb rupture failure criterion (equation 2). Carter and Kulhawy (1988) also note that equation 25 closely resembles that by Bell (1915) as seen in equation 9. O'Neill and Reese (1999) have developed an empirical method to calculate bearing capacity from the Hoek and Brown (1980) solution as follows:

[26] $$q_t = \alpha q_u$$

where:

[27] $$\alpha = [s^{0.5} + (ms^{0.5} + s)^{0.5}]$$

The values for the terms "m" and "s" in this equation can be found in Table 2 and Table 3 depending on rock type and description. Usually equation 26 is not seen in the form listed with the term α, however this term has been introduced in this manner as a simple way of investigating this central term to compare this method to that of Rehnman and Broms (1971). These values of "α" that were evaluated by the author can also be seen in Table 3.

Table 2 Rock description (after O'Neill and Reese, 1999).

Rock or Intermediate Geomaterial Type	Description
A	Carbonate rocks (e.g. dolostone, limestone, marble)
B	Lithified argillaeous rocks (e.g. mudstone, siltstone, shale, slate)
C	Arenaceous rocks (e.g. sandstone, quartz)
D	Fine grained igneous rock (e.g. andesite, dolerite, diabase, rhyolite)
E	Coarse grained igneous and metaporphic rock (i.e. amphibole, gabbro, gneiss, granite, norite, quartz diorite)

Table 3 Values for m and s for rock description (after O'Neill and Reese, 1999).

Quality of Rock	Joint Description	Joint Spacing	S	m (α) Type A	m (α) Type B	m (α) Type C	m (α) Type D	m (α) Type E
Excellent	Intact	>3m	1	7 (3.83)	10 (4.3)	15 (5)	17 (5.23)	25 (6.1)
Very Good	Inter-locking	1-3m	0.1	3.5 (1.41)	5 (1.61)	7.5 (1.89)	8.5 (1.99)	12.5 (2.33)
Good	Slightly Weathered	1-3m	$4x\ 10^{-2}$	0.7 (0.62)	1 (0.69)	1.5 (0.78)	1.7 (0.82)	2.5 (0.93)
Fair	Moderately Weathered	0.1-1m	10^{-4}	0.14 (0.05)	0.2 (0.06)	0.3 (0.07)	0.34 (0.07)	0.5 (0.08)
Poor	Weathered	30-50mm	10^{-5}	0.04 (0.01)	0.05 (0.02)	0.08 (0.02)	0.09 (0.02)	0.13 (0.02)
Very Poor	Heavily Weathered	<50mm	0	0.007 (0)	0.01 (0)	0.015 (0)	0.017 (0)	0.025 (0)

As can be seen above in Table 3 above, Rehnman and Broms (1971) is only comparable to Hoek and Brown (1980) for rock qualities considered "excellent". For any rock qualities weaker than "excellent", this "α" is significantly smaller than the Rehnman and Broms (1971) range.

2.4 Field Measurement Of Pile Toe Capacity

2.4.1 Pile Load Testing

Quality assurance is an integral part of any engineering project and the same holds true in pile driving projects. On typical pile driving projects, at least one pile is tested to ensure that its resistance is at least greater than the resistance for which it has been designed. Static load testing is the most reliable method to measure pile capacity, but it is also an expensive and time consuming method (CFEM, 2006). Whitaker (1976) explains the various pile load testing methods available. Usually a known load is applied in stages via a hydraulic jack and the vertical deformation of the pile is recorded for each increase of load. Depending on the specification for the project, the pile will be loaded to some factor above the design load or loaded to its ultimate capacity.

There are many different ways to interpret the ultimate capacity of a pile from a load test. One such interpretation method developed by Davisson (1973) is known as the offset limit load. This offset distance can be seen in equation 28, as described by Fellenius (2011).

[28]

$$x = 4 + \frac{B}{120}$$

Where:

x = horizontal offset movement from initial elastic portion of load deflection curve (mm)

B = pile base diameter (mm)

This is the horizontal offset from the initial slope of the elastic portion of the load (P) versus pile base movement (Δ) curve for the load test which is given by equation 29.

[29] $$P = \frac{AE}{L}\Delta$$

Where:

P = pile load (F)

E = elastic modulus of pile (P/L^2)

Δ = movement of pile base (L)

A = cross sectional area of pile (L^2)

L = length of pile (L)

The ultimate load of the pile is defined by where this offset line passes the load-movement curve as seen in Figure 3. As noted from this figure, it is important to load the pile to adequate vertical deformation to ensure the pile has mobilized its full resistance. As you can see in Figure 3, if the displacement (or movement) was not large enough, the ultimate load resistance could not have been determined.

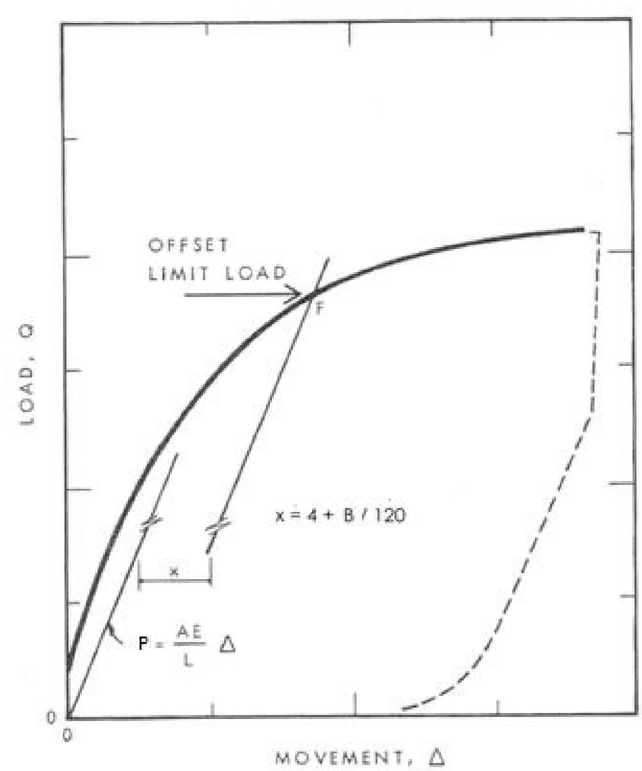

Figure 3 Sample Davisson method plot (CFEM, 2006)

There are many other methods that can be used to determine pile load capacity by interpreting pile load testing results. Fellenius (1980) provides a comparison of these methods.

2.4.2 Pile Driving Analyzer (PDA)

A common way of estimating the ultimate capacity of a pile is via a Pile Driving Analyzer (PDA). When the pile driving hammer makes contact with the pile, the stress wave from the impact is transferred through the pile in the form of a compressive strain wave (Fellenius, 2011). This wave propagates through the pile at the speed of sound until it arrives at the pile toe (Fellenius, 2011). When encountering the pile toe, the wave is then reflected back up the pile. The displacement of the pile as a result of this wave propagation can be described using the one dimensional wave equation in the form of a double derivative as found in Coduto (2001) and as shown below in equation 30:

[30]
$$\frac{\delta^2 u}{\delta t^2} = \frac{E}{\rho}\frac{\delta^2 u}{\delta z^2}$$

Where:
z = depth below ground surface (L)
t = time
u = displacement of the pile at depth z (L)
ρ = density of pile material (M/L^3)

There are many interactions that can influence the development of the wave as it transfers through the pile. This may include that between the hammer, cap and pile and those between the soil and pile. These lead to very complex boundary conditions associated with pile driving. Coduto (2001) discusses the steps that Smith (1962) took to develop numerical methods for solving the wave equation in equation 30, taking into consideration all of these factors. Smith (1962) separated the individual elements of the pile driving system into a series of weights, linear dashpots and springs, as shown in Figure 4. The constant known as quake (Q) describes the displacement of the soil required to mobilize full plastic resistance of the spring (Fellenius, 2011). The Smith damping factor (J) can be described by the linear relationship between the dashpot resistance and the velocity (Coduto, 2001). Graphical representations of quake and Smith damping can be seen in Figure 5.

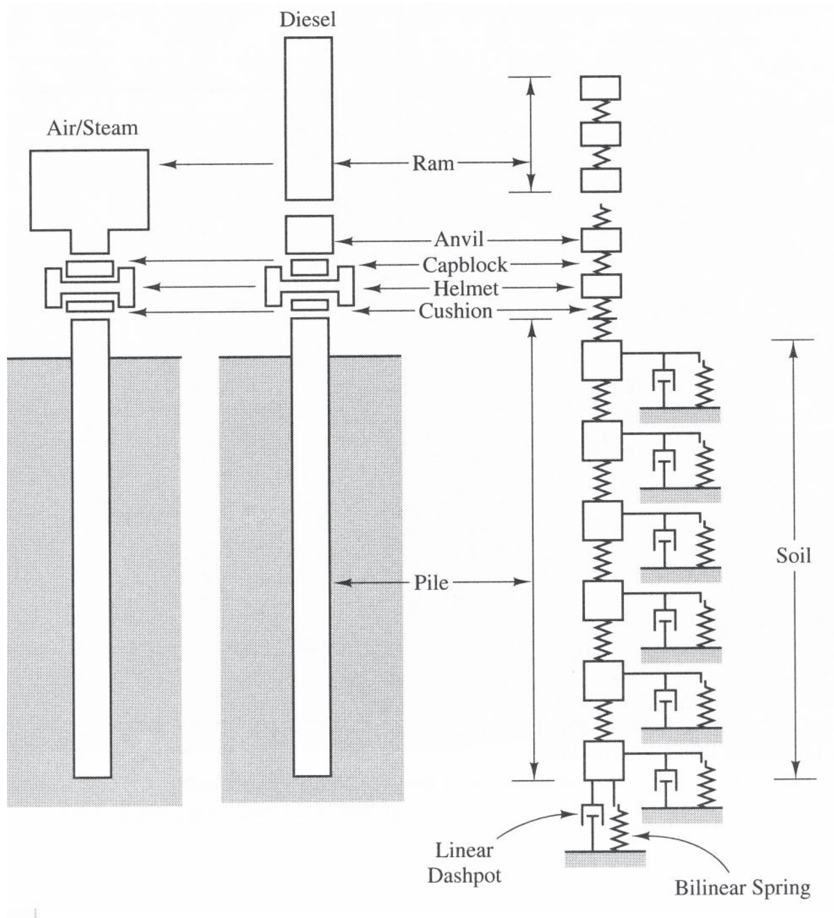

Figure 4 Smith numerical methods model (Coduto, 2001)

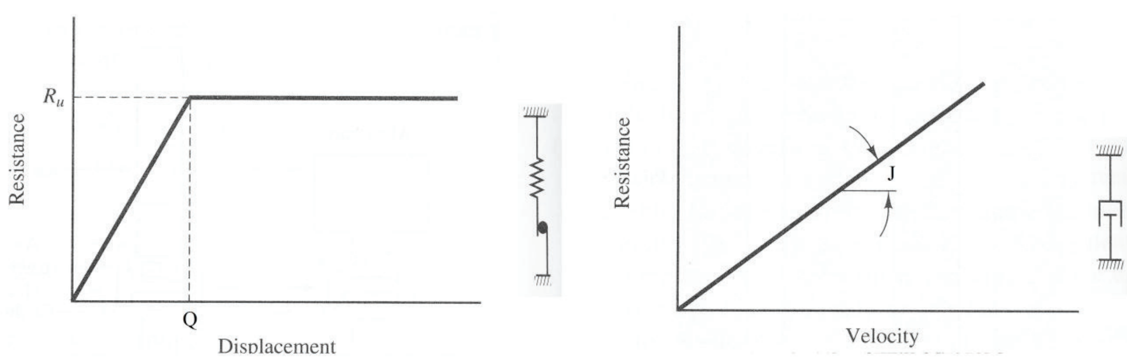

Figure 5 Graphical explanation of quake and Smith damping (Coduto, 2001)

This pile driving wave theory can be analyzed using pile driving analyzer (PDA) technology along with the computer program PDA-W in order to measure pile resistance (Pile Dynamics, Inc., 2004). Setup and running a PDA test takes minimal time compared to pile load testing methods. PDA is comprised of a series of accelerometers and strain gauges which are attached to the pile. These gauges are then connected to a computer on site that is used to record these gauges during the pile driving process. As described by Fellenius (2011), the gauges are able to read both the force and velocity wave propagation through the pile for each blow of the hammer. An equation derived directly from the one dimensional wave equation specific for pile driving, as found in Fellenius (2011), can be seen below in equation 31, while equation 32 defines the velocity of the compressive wave. The force and velocity waves are related through a pile material constant called impedance, as shown in equation 33 (Fellenius, 2011). The definition of pile impedance itself is described in equation 34 (Fellenius 2011).

[31]

$$\sigma = \frac{E}{c_v} v$$

Where:

v = particle velocity in pile (L/t)

σ = stress in pile (F/L^2)

c_v = velocity of compressive wave in pile (L/t)

and:

[32]

$$c_v = \sqrt{\frac{E}{\rho}}$$

[33] $$F = Zv$$

Where:

F = force in pile (F)

[34] $$Z = \frac{EA}{c_v}$$

Where:

Z = pile impedance (F*t/L)

Plots of the measured velocity and force wave versus time can be uploaded to PDA-W for each hammer blow in the pile driving process. These wave trace plots assist in describing resistances within the pile. A key time on these plots is $2L/c_v$, which is the time it takes for a wave to travel to the toe of the pile and be reflected back. An example of these wave traces can be found in Fellenius (2011) and from Hannigan (1990), as shown in Figure 6. These three different plots show wave movement through three different types of piles. The top plot shows a case with minimal shaft or toe resistance, which would describe a pile in the early stages of pile driving. The second plot demonstrates a pile with large toe resistance; this is represented by a large spike in the force wave at time $2L/c_v$. The bottom plot displays a pile with large shaft resistance which is evident by a gradual buildup in the force wave before the time $2L/c_v$ because the wave is being reflected as it travels down the pile.

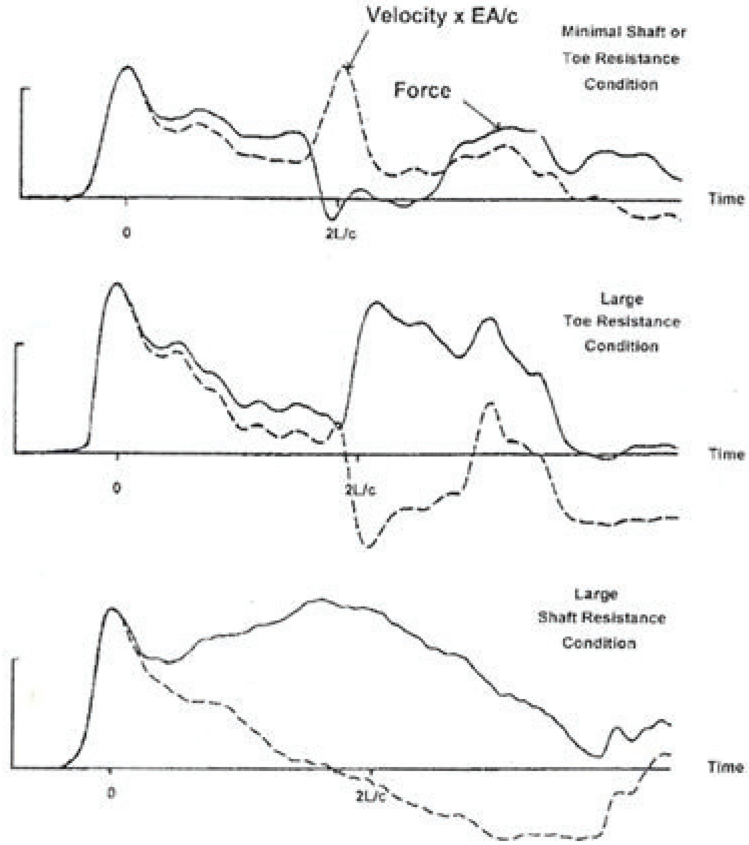

Figure 6 Sample PDA-W wave plots. (Hannigan, 1990).

2.4.3 Case Pile Wave Analysis Program (CAPWAP)

For more detailed results, PDA-W files can be analyzed through a program called Case Pile Wave Analysis Program (CAPWAP) by Pile Dynamics Inc. (2000) to break down a more precise estimation of ultimate pile resistance, including shaft and toe resistances. This analysis cannot be properly performed in the field as it requires a complete PDA-W file to perform.

For this program, a single wave plot from the series of PDA-W plots is selected. This plot should be a good representation of the overall data collected for the period of interest (Pile Dynamics, Inc. 2000). The purpose of using PDA-W is to present a plot of the measured waves travelling through the pile for each strike of the hammer. CAPWAP presents the best match of a theoretical wave plot (by solving the equation with the appropriate boundary conditions) to the measured wave plot (Pile Dynamics, Inc., 2000). A sample of a plot with good matching data can be seen below in Figure 7. In this plot, the solid line represents the measured force plot from PDA-W while the dotted line is the theoretical plot developed in CAPWAP.

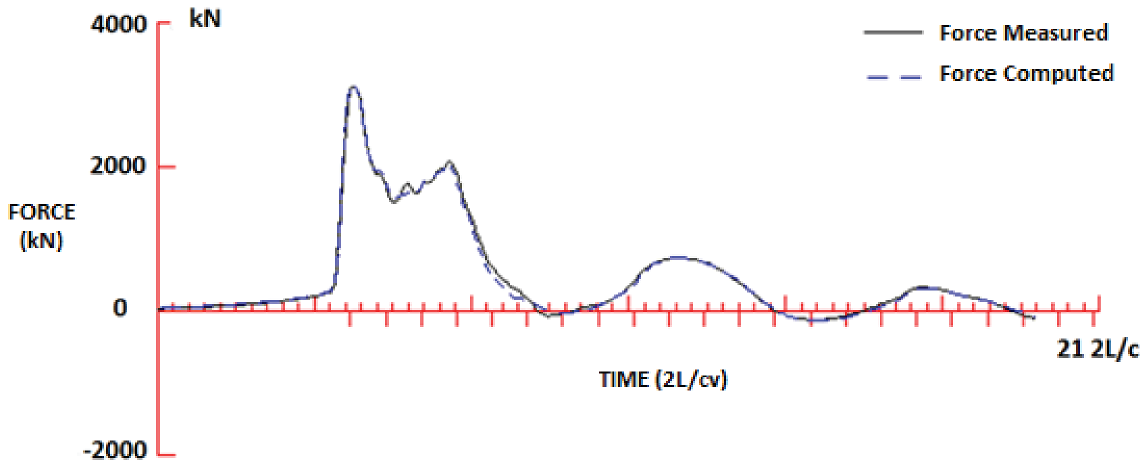

Figure 7 Sample CAPWAP plot matching

Attempting to achieve the best wave plot match in CAPWAP is an iterative process. Once the initial estimated values for shaft resistance have been entered, initial values for quake and damping must be estimated. The goal is to attain the best match quality possible, where the match quality is a number describing the overall match of all plots associated with the wave data (Pile Dynamics Inc., 2000). The estimated shaft and toe resistance along the pile must be changed along with a series of parameters used to describe the wave propagation. In the software, a list of CAPWAP variables are varied within limits as a means to provide a best fit in the plot matching process. This process should begin by altering the damping and quake constants, because these parameters have the largest effect in the first $2L/c_v$ of the wave plot (Pile Dynamics Inc., 2000).

An interesting study comparing predictive pile capacity methods was performed by Long et al. (2002). This study compared the accuracy of many different methods of estimating pile capacity. It compares these methods for both end of initial drive (EOID) and beginning of restrike (BOR) conditions. Driven steel piles are often monitored at two different stages of driving. Initial driving is used to monitor pile integrity and stress changes during driving while restrike driving provides a much more relevant estimate on pile toe capacity (Fellenius, 2011). The methods analyze in Long et. al. (2002) included pile driving formulas, PDA, CAPWAP and other wave equation analysis methods. Long et al. (2002) examined various data sources to create plots of measured (i.e. from pile load tests) versus predicted resistances for each of the estimation methods, for both initial drive and restrike conditions. For initial drive conditions, PDA, CAPWAP and two other wave equation methods measured the pile capacity at nearly the same accuracy, all under-predicting capacity by an average of 44 to 46 percent. When restrike conditions were considered however, CAPWAP was the best at measuring actual pile capacity.

2.4.4 Factors Affecting PDA Field Measurements

An article by Rausche et al. (1985) discusses the dynamic wave mechanics in pile driving and how it is expanded through the program CAPWAP. In this article, the combined usage of PDA with CAPWAP is compared to static load testing. This article discusses CAPWAP results, saying that the pile resistance must be fully mobilized during driving to properly measure the ultimate pile resistance. This means that the hammer being used must provide an energy sufficiently large enough to mobilize the entire pile. For example, if the energy subjected by the hammer is too small, the pile may be able to resist the entire load of the blow and additional load and result in no movement. The Federal Highway Administration (FHWA, 2006) also mentions this criteria and states that because pile resistances are often not fully mobilized, CAPWAP ultimate load data tends to be conservative and the pile ultimate loads are often much higher. Both of these publications suggest that a pile may not be fully mobilized is if it takes more than 10 hammer blows to drive the pile 25mm.

One other technical aspect of pile driving that must be considered is the differentiation between EOID and BOR pile driving results. A problem associated with measuring pile resistance with the use of PDA is relaxation or setup. CFEM (2006) discusses the causation and problems associated with relaxation. Relaxation can occur in non-cohesive silts and dense sands because pile driving induces negative pore water pressures. These negative pore pressures can cause the soil to dilate, causing apparent increases in measured pile resistances over time. Once these pore pressures dissipate, these resistances can become much smaller. This dilation has a more significant effect on smaller piles than larger piles (Randolph and Gourvenec, 2011). Morgano and White (2004) discuss that this same phenomenon can occur in piles driven to rock. Morgano and White (2004) found that tested piles lost up to 50% of their strength from initial drive to restrike. For this reason it is highly recommend that piles in highly weathered soft rock be tested by restrike a minimum of 1 to 3 days after the initial drive. Also, only the first few hammer blows should be considered for PDA measurements. There are also circumstances where the soil surrounding a pile can actually become stronger over time; this process is called set-up. CFEM (2006) explains that set-up can occur in saturated sands and silts through temporary liquefaction. This liquefaction can be induced by pile driving and reduces the driving resistance of the pile. Randolph and Gourvenec (2011) explain that this phenomenon can also occur in soft clays where excess positive pore water pressures can surround the pile. In both cases, the ultimate pile resistance increases with time as the pore water pressures dissipate. According to Axelsson (2002), set-up can occur for years and has a rate of about 40% per log cycle of time.

2.5 Summary and Conclusions

Several empirical and theoretical methods associated with estimating the ultimate toe capacity of steel driven piles have been discussed in this chapter. Only one method (Rehnman Broms, 1971) was found to estimate the ultimate base capacity of steel driven piles. However, there were several methods found to predict the ultimate toe capacity of drilled sockets. These methods include those by Bell (1915), Coates (1981), Rowe and Armitage (1987), Zhang and Einstein (1998), Ladanyi and Roy (1971) and Hoek and Brown (1980). It is believed by the author that these methods are applicable because of the common nature of steel driven piles and drilled sockets, however the relationships for sockets will likely prove to be more conservative when applied to small displacement driven steel piles. This comes from the fact that the bases of drilled sockets tend to be affected more by the presence of rock discontinuities.

This chapter also investigated the different manners that pile capacities can be measured in the field. It was discussed that static load testing is the preferred industry standard, but due to financial and time constraints that methods using wave analysis, including the usage PDA-W and CAPWAP, are considered acceptable in practice and referenced in many design codes and foundation design manuals.

CHAPTER 3 DATA COLLECTION

3.1 Data Collection Requirements

As stated in Chapter 1, the purpose of this thesis is to use actual PDA data to develop toe capacity prediction methods for driven steel piles to rock. This process involved the review of hundreds of geotechnical and PDA reports from Stantec Consulting Ltd. in Dartmouth, NS. For this thesis, it was determined that quality data would be valued for this research over quantity. This required the development of a defined data collection procedure. Data that did not meet minimum requirements were not used in the formulation of the work. As will be shown in this chapter, the result of these minimum "standards" was a reduced amount of data to examine.

A three step data collection process was developed to carry out the research presented in Chapter 4. The three steps of data collection are described below in the order that they were normally completed. The data collection process worked most efficiently when followed in this order, as it represents the hierarchy of importance in this data collection method.

3.1.1 Pile Type and End-Bearing Conditions

The focus for the research was small displacement, steel piles, so only sites using steel driven H-piles and open ended steel pipe piles were considered. It was also required that piles on these sites were driven to rock. The rock conditions were generally of the weaker variety (i.e. sedimentary) to ensure full pile mobilization. This included sites with mudstone, shale, slate, gypsum or sandstone bedrock conditions.

3.1.2 PDA Report Requirements

The first step in data collect was to obtain past PDA reports for various job sites containing small displacement, driven steel piles. Reports considered "acceptable" for data collection provided details of all piles that were tested on the sites. Each pile tested was listed by the pile name, type and size. Information on the hammer being used and the energy put into the pile driving process were also included. The amount of blows per

25 mm was considered an important piece of information in these reports because piles of approximately 15 blows (or fewer) per 25 mm of pile penetration into rock were considered fully mobilized. Garland Likins, a specialist in pile dynamics and one of the co-authors in Rausche et al. (1985), was contacted. He stated that "the 2.5 mm (per) blow is only guidance, and not an absolute limit. But it is reasonable that CAPWAP would be a lower bound solution at very high resistances" (Likins, pers. com. 2011). It was decided that a cutoff of 15 blows per 25 mm was sufficient.

Another important piece of information taken from the PDA reports were the measured shaft and toe resistances measured from using CAPWAP. Knowing the toe resistance in relation to the shaft resistance was also a good initial indicator of whether or not the pile was driven to rock. As discussed in Chapter 2, since multiple sources (e.g. CFEM, 2006) suggested that piles should be re-tested because of potential changes in pile resistance over time, only piles tested under restrike conditions were considered for this project. For some sites, PDA-W analysis had been completed, yet CAPWAP was not carried out; for these sites CAPWAP was completed using the PDA-W data by the author for the sake of this project. The results of these analyses are provided in Appendix A.

The location and depth of the piles selected were also necessary for the use of PDA data. Only piles with a listed value for pile toe elevation were selected. Since grade level changes frequently throughout the life of a project, PDA reports that only listed pile driven depths were not included because it was unclear as to the exact location of the pile toe. It was also a requirement that all PDA reports include a pile location map or contained detailed information on the pile locations so that the location of each pile on the site was evident. Individual pile driving records describing blow count information with varying depth in the pile driving process were not a requirement, but were helpful in determining the depth to which the pile was driven into the rock.

3.1.3 Geotechnical Site Investigation Requirements

For sites with "complete" pile information and toe bearing conditions, as well as PDA files, geotechnical site investigation reports had to be found for the corresponding job sites. Many of the job sites had companies other than Stantec complete these reports meaning that these reports were not always readily available. There were also other sites on which only very limited geotechnical site investigations were carried out. On some of the smaller PDA job sites, no site investigations were completed. Having a geotechnical site investigation is very important for the knowledge of the site geology at the toe of the driven pile. Geotechnical site investigation reports contain all borehole data, giving details of the soil layers and details of the rock at the pile toe. Soil and rock elevations, detailed descriptions of the rock type and RQD values are all given in this borehole data. In some of the larger sites, unconfined compressive stress tests were also carried out, which would define the strength of the rock in each borehole.

It was also a requirement that borehole locations be well documented for a job site for the data to be included in the research. Data was not useful if the PDA data and geotechnical site investigation could not be linked since it is unknown whether or not the pile penetrates the bedrock (and to what degree). Rock type and depth often changes throughout a particular site so matching piles with boreholes in the same proximity was essential to ensure proper data collection.

Geotechnical site investigation reports often include results from unconfined compressive strength tests; however in some cases these tests were never performed. If unconfined compressive stress tests were not carried out, an estimate of the unconfined compressive stress made from point load test was deemed sufficient. A large portion of the site reports reviewed had completed neither of these tests, so if the rock cores were still in the basement at Stantec Consulting Limited, an unconfined compressive strength test was carried out if a core of acceptable length could be retrieved (ASTM D7012-10, 2010). If insufficient core length could not be obtained, the standard for point load testing (ASTM D5731-08, 2008) was performed and the unconfined compressive stress was determined with the results. Unfortunately there were many cases where unconfined compressive strength data was lacking and no rock cores were available. As most pile toe capacity estimates are based on unconfined compressive strength of the rock, it was decided that sites without unconfined compressive strength testing would not be used in the research.

The schematic in Figure 8 summarizes the process that was used in order to collect data as outlined in the previous sections of the report.

	Selection of Pile Type and Conditions	PDA Report	Geotechnical Site Investigation
Required	• Steel H-Piles or steel open ended pipe piles • Pile must come into contact with rock	• Measured toe resistance • Pile toe elevation • Pile location on site (pile map) • Blows per 25 mm • Pile type and size	• Unconfined compressive strength • RQD • Rock profile, elevation and type • Borehole locations
Other	N/A	• Measured frictional (shaft) resistance • Details on hammer type • Hammer energy • CAPWAP damping and quake constants • Pile driven depth	• Soil stratification • Weathering/ fractures descriptions • SPT N values of soil • Depth of water table • Other specific soil and soil testing details

Figure 8 Data collection stages.

3.2 Selected Site Data

Pile data analyzed was not restricted to any certain type of construction project, however the majority of the projects used were bridge, overpass or interchange projects. This is mainly due to these projects using pile based foundations more frequently. Other projects used contained commercial and municipal building foundations. Table 4 below displays all required parameters for each job site. A checklist of the required parameters for some of the analyzed sites considered for this database can be seen in Appendix B.

Table 4 Selected Pile Details

Site	Number	Pile Type	Base Area (m^2)	Base Width (m)	Shaft Area (m^2/m)	t (m)	Hammer Energy (kJ)
1	1056734	OEPP 324X9.5	0.00939	0.324	1.018	0.0095	18-25
2	1017681	HP 360X132^	0.03114	0.360	2.154	0.0156	31-38
		HP 360X132	0.01690	0.360	2.154	0.0156	31-38
3	121612385	HP 360X152	0.01940	0.36	2.172	0.0179	28-37
		HP 360X152	0.01940	0.36	2.172	0.0179	28-37
		OEPP 508X12.7	0.01976	0.508	1.596	0.0127	28-37
		OEPP 508X12.7	0.01976	0.508	1.596	0.0127	28-37
4	1046136	HP 12X74	0.01406	0.31	1.827	0.0155	34-40
5	121613582	HP 360X152	0.01940	0.36	2.172	0.0179	23-29
6	121613585	HP 310X110	0.0141	0.31	1.826	0.0154	9-11
7	121611479	HP 310X110	0.0141	0.31	1.826	0.0154	36-42
		HP 310X110	0.0141	0.31	1.826	0.0154	37
8	7892J	HP 310X132	0.01670	0.31	1.843	0.0183	27-37
9	121910609	HP310X79	0.01000	0.31	1.804	0.0110	24-42
10	121614157	HP310X110	0.0141	0.31	1.826	0.0154	26-35

^Pile included steel welded plates in addition to the pile size.

Table 4 continued.

Site	Number	Shaft in Rock* (m)	RQD (%)	Shaft Resistance (kN)	Toe Resistance (kN)	blows/ 25mm	q_u (MPa)	Core Rec.# (%)
1	1056734	0.15	62	589	736	5	8	5
2	1017681	7.5	13	1482	1736	9	10	100
		4	13	2729	950	12	10	100
3	121612385	2.15	61	984	2077	12	18	81
		2.59	17	880	1973	12	8.5	45
		1.36	62	228	2469	9	14.3	100
		1.26	76	617	3180	15	14.3	100
4	1046136	2.2	64.5	761	1205	15	8	100
5	121613582	7.03	41.1	1492	894	8	16	100
6	121613585	0.52	17	487	791	13	5.4	40
7	121611479	1.95	38.5	1715	915	10	9.9	93
		6.91	1	1409	967	12	8.1	4
8	7892J	0	79	983	2057	13	10	-
9	121910609	3.7	70	1338	762	8	10.8	95
10	121614157	0.66	11	1471	1440	13	15	40

*Shaft in rock is elevation of rock face minus pile toe elevation

#Core recovery % is length of core recovered divided by total rock depth

Table 4 continued.

Site	Number	Rock Description
1	1056734	Very weak/soft slightly fractured reddish brown sandstone
2	1017681	Very severely fractured weak fresh dark grey shale (completely weathered top meter)
		Very severely fractured weak fresh dark grey shale (completely weathered top meter)
3	121612385	Poor to good quality red sandstone.
		Very poor to poor quality red sandstone.
		Poor to good quality red sandstone.
		Poor to good quality red sandstone.
4	1046136	Poor to fair quality, slightly weathered light brown sandstone/mudstone
5	121613582	Fair to good quality, slightly to highly weathered mudstone.
6	121613585	Moderately to highly weathered, moderately to highly fractured mudstone. Poor quality.
7	121611479	Moderately fractured, low strength, white-grey Gypsum/Anhydrite.
		Highly fractured, very low strength, light grey mudstone.
8	7892J	Reddish brown medium to coarse-grained weak to medium strong sandstone
9	121910609	Very weak fine grained reddish brown sandstone interbed w/ hard reddish brown mudstone
10	121614157	Very poor to poor brown mudstone.

Table 4 continued.

Site	Number	BOR/EOID	CAPWAP?	Notes
1	1056734	BOR	Yes	Only one [illegible] BHs to east of hanger. Average strength of unconfined test.
2	1017681	BOR	No	Pile drivi[illegible]ys nearest BH2. Pile has steel welded plates added to it.
		BOR	No	Pile driving record says nearest BH2.
3	121612385	BOR	Yes	North Abutment. Used BH 1 and BH 8 data.
		BOR	Yes	South Abutment. Used BH 4 and BH 5 data. Only in mudstone.
		BOR	?	Pier. Used BH 7 data.
		BOR	?	Pier. Used BH 3 and BH 6 data.
4	1046136	BOR	Yes	Used BH 2 & BH 3.
5	121613582	BOR	?	Assumed BH 8.
6	121613585	BOR	Yes	Between BH 1 and BH 2, closest to 2.
7	121611479	BOR	Yes	Nearest to BH 9. Used Maritime Testing BH log.
		BOR	Yes	Nearest to BH 4. Used Maritime Testing BH log.
8	7892J	BOR	No	BH 109.
9	121910609	BOR	No	Used average of BH 101 and BH 103 (almost exactly halfway between)
10	121614157	BOR	Yes	Used BH 2.

3.3 Summary and Conclusions

A screening process has been developed and presented for determining "good" quality data for the further analysis of the approaches discussed in Chapter 2. As discussed, over 100 pile projects were assessed for potential inclusion in the database to be used for this research. After following the screening procedure adopted, only 15 pile records were selected to be used in the data base. A comparison of these "high quality" measured pile predictions will be used in the following chapter to compare to the various pile prediction methods presented in Chapter 2.

CHAPTER 4 RESULTS AND DISCUSSION

4.1 Analyzing Direct Empirical Design Methods

Methods to predict toe capacity of piles in rock found in the literature review have a common theme; there is some direct relationship of the ultimate pile toe capacity to the unconfined compressive strength of the rock. The method proposed by Coates (1980) is based purely on rock mechanics for drilled sockets but involves a simple linear relationship to the unconfined compressive strength of the rock. Another relationship by Rowe and Armitage (1987) is developed based on static load testing of drilled sockets found in the literature. A third method reviewed, that was proposed by Rehnman and Broms (1971) is the only one of these three methods that is specific to driven piles.

In order to assess the appropriateness of these various methods to predict toe capacity for driven small displacement piles on rock based on simple relationships to unconfined compressive strength of the rock, the data that met the filtration criteria described in Chapter 3 was used. The unconfined compressive strength of the rock was plotted versus measured toe resistance from PDA records for each of the driven low displacement steel piles. A linear regression through the origin was then fit to this data. The slope of this line is given as η in equation 35 below:

[35] $$q_t = \eta q_u$$

Since the data from the PDA files display the pile toe resistance in the form of a force, all resistances were divided by the net steel pile toe area. For the best fit line developed for this data set, a series of confidence intervals were also plotted for this data to provide a qualitative assessment on how reliable the data is relative to the best-fit line. The plot developed for the data set, including a best fit line and different confidence intervals (95%, 98%, 99.9% and 99.99%) can be seen in Figure 9. Manual calculations of the regression analysis using the method in Mendenhall and Sincich (1996) were performed as a check on the Microsoft Excel© generated regressions.

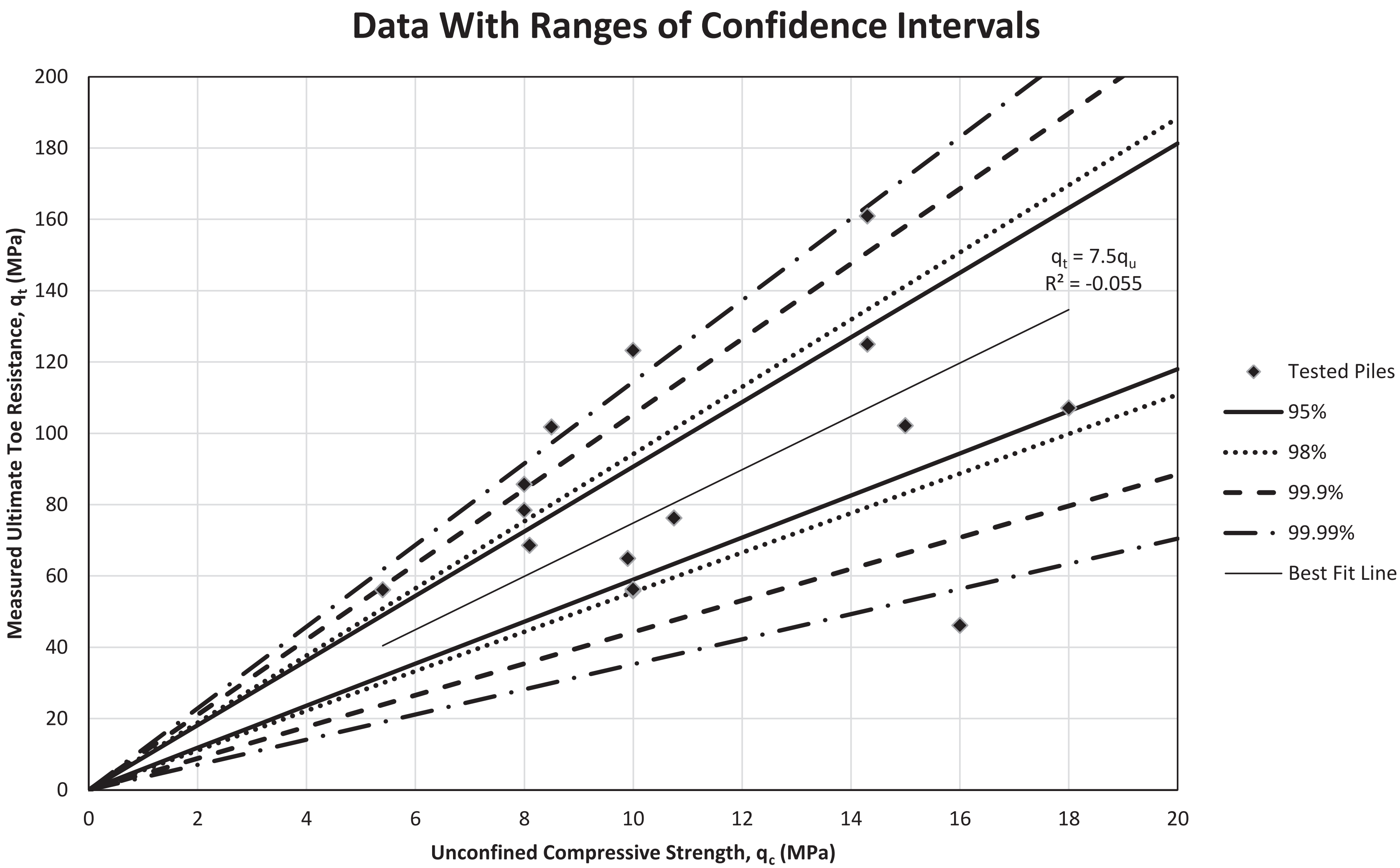

Figure 9 Data set containing confidence intervals

Examining Figure 9, a “η” value of 7.5 is the slope of the best fit regression line through the data. The R^2 value for this best fit is not surprising poor, given the scatter and limited amount of data used in the regression. To further analyze the variability of the data, various confidence intervals were calculated for the fit of the data. Confidence intervals are shown in Figure 9 for increasing levels of confidence. The slopes (i.e. “η”) of these lines are provided in Table 5 to provide an estimate of upper and lower bounds to the fits of the regression at the different confidence levels. It is evident that one data point (16, 46) tends to skew not only the best fit line of the data, but also the confidence intervals. This also leads to some of the higher values of “q_t” residing outside of the 99.99% confidence interval although they tend to coincide with the majority of the rest of the data. This outlying data point (16, 46) comes from site number 121613582. The data collection process outlined in Chapter 3 provides no reason to remove this data point and hence it remained in the data set. Although the entire rock core was recovered for the borehole for this pile, the geotechnical site investigation states that the majority of the recovered rock was too weathered to be tested and that zones of weaker rock may have been encountered. This means that this outlier may exist simply because the rock core tested was not representative of the rock on site. If anything, this data point provides a reminder of the nature of empirical design methods and how even lower bounds can be exceeded in some cases. It is apparent however, that the 98% confidence limits “envelopes” the lower bound data with the exception of this point.

Table 5 Confidence interval slopes for best fit of data set

Interval (%)	Lower Bound	Upper Bound
95	5.9	9.1
98	5.5	9.4
99.9	4.4	10.5
99.99	3.5	11.4

Comparing the slopes of the upper and lower bound confidence limits to the literature relationships discussed earlier provides some context between the result of the PDA results in this study and the studies presented in the literature. A plot of the data, along with the 99.99% confidence limits can be seen in Figure 10. On this plot, there are lines representing Coates (1981) and Rowe and Armitage (1987) as well as three lines for Rehnman and Broms (1971) (one for a factor of 4, 5 and 6 respectively) to compare these methods to the best fit of the data.

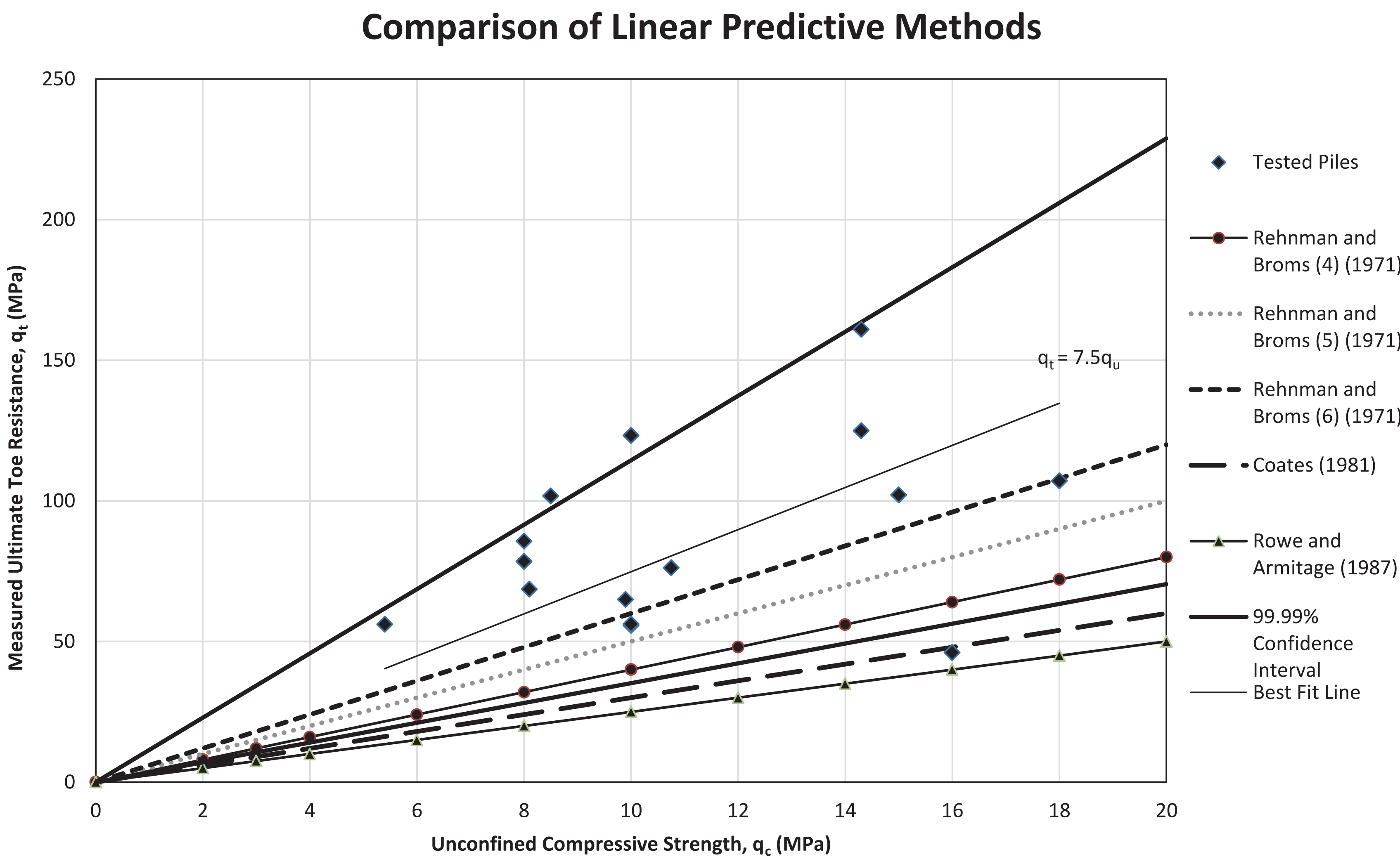

Figure 10 Comparison of direct empirical methods

Figure 10 shows that the best fit value of "η" of 7.5 obtained from the regression analysis is much higher than all of the empirical methods discussed; the closest method is that of the upper value of 6 suggested by Rehnman and Broms (1971) for granite rocks. The studies by Rehnman and Broms (1971) had minimal penetration of the steel pile into the rock sample and hence the results from this investigation where some embedment of the pile toe into the rock would result in slightly higher values.

When considering the 99.99% confidence interval in Figure 10, Coates (1981) is on the conservative side of this lower interval. Rehnman and Broms (1971) with a factor of 4 is slightly above this same confidence interval. Lastly, it can be seen that Rowe and Armitage (1987) is the most conservative in comparison to the other methods for this data set. It is not surprising that this method is conservative. As mentioned in Chapter 2, this is an empirical method for drilled sockets. Since socketing into rock tends to be effected more by rock discontinuities, it was expected that this methods would be conservative when applying them to low displacement, steel driven piles. Since Rowe and Armitage (1987) was based on the results of pile load testing that was not completed to failure, it was expected that it would be very conservative. Coates (1981) is also conservative in all cases, but may be the most appropriate method when considering the extreme case of the 99.99% confidence interval.

4.1.1 Considering a Power Function Best Fit Line

The method proposed by Zhang and Einstein (1998) is based on the best fit of a collection drilled sockets found in literature but also utilizes a power curve fit to the field data. To examine the applicability of this method, a power function was used to represent the best fit of the data set. The data points were placed on a logarithmic scale and were fitted with a best fit relationship as follows:

[36] $$q_t = \eta q_u{}^{\upsilon}$$

The fit of this line as well as the parameters for the power fit suggested by Zhang and Einstein (1998) are plotted in Figure 11. Other methods as shown by the legend on Figure 11 were also plotted for comparison.

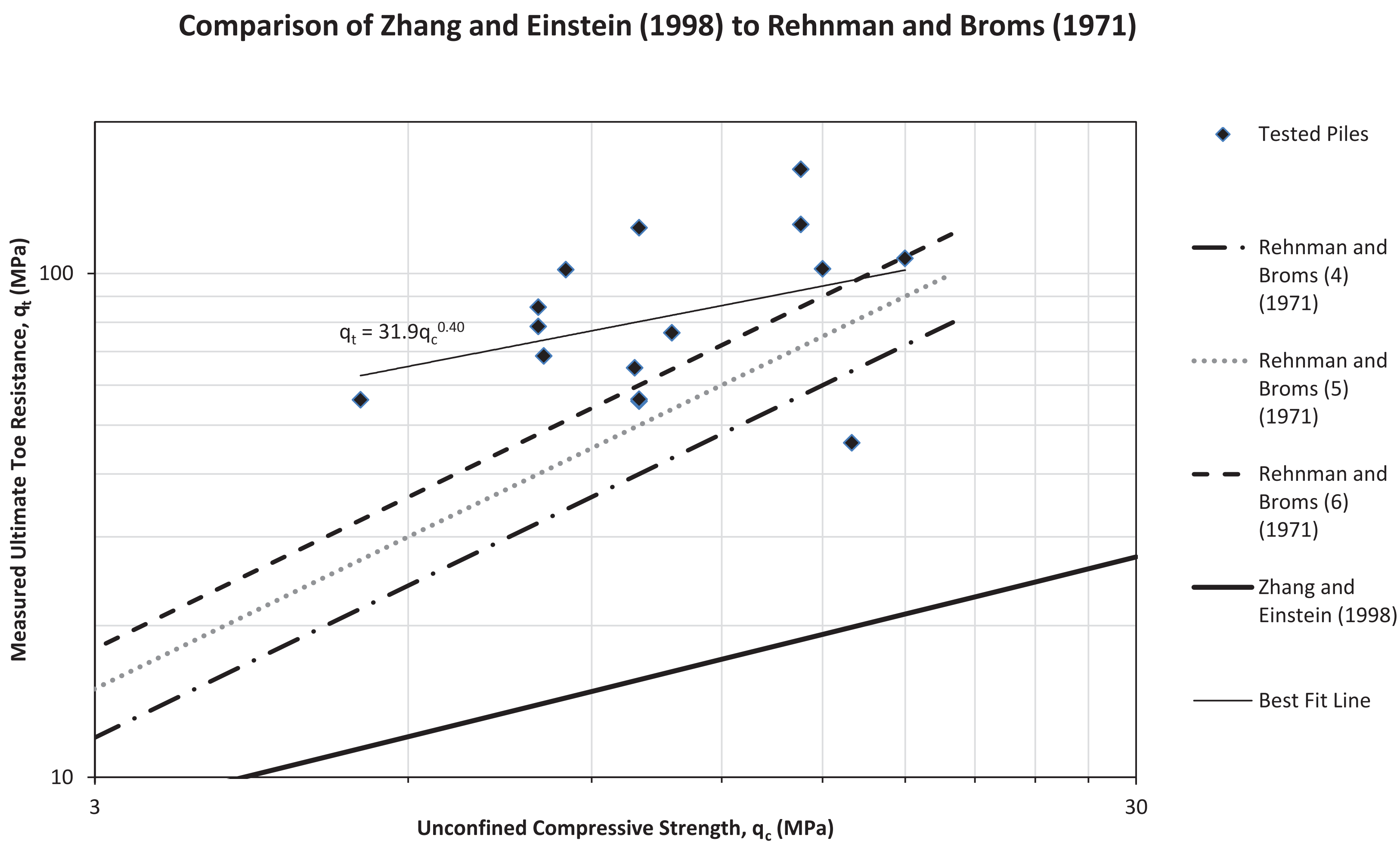

Figure 11 Comparing Zhang and Einstein (1998) and Rehnman and Broms (1971)

While examining the power fit to the data set as completed in Figure 11, it was found that a "η" of 31.9 and a "υ" value of 0.40 provide the best fit, although it appears that this data set does not conform well to this type of fit. Figure 11 shows that Zhang and Einstein (1998) tends to greatly underestimate the ultimate pile toe resistance for driven steel piles and that Rehnman and Broms (1971) is a much better representation of the data.

4.1.2 Analyzing Hoek and Brown (1980) Empirically

For analysis purposes, Hoek and Brown (1980) is a slightly different case than those described above. This method is very highly dependent on the aperture of discontinuities. Discontinuity aperture is a parameter that the author had no access to and had no means of estimating. For this reason, there was no way to calculate pile toe resistances using this equation with the data obtained. However, it was possible to evaluate this method through the calculated values of "α" that were determined in Chapter 2 in Table 3. Using Table 2 with Table 4, it can be seen that all rock types for piles used in the data base can be classified as rock types A, B and C. In Table 3, "excellent" rock quality for these types of rock exhibit "α" values that range from 3.83 to 6.1. When comparing these values to the confidence intervals in Figures 9 and 10, these values match up quite well with what would be desired for an estimated pile toe capacity method with this data set. However, Table 4 shows that the rock descriptions for this data base range from "very poor" to "good" since these rocks contain a varying degree of weathering. This means that according to rock descriptions available for these sites, the "α" values should be between 0 and 0.93 for all of these points, so this method would give conservative toe resistances for the data presented. Since rock discontinuities tend to have less effect on the toe resistance of driven steel piles than on drilled caissons, it is possible that when using this method for small displacement, driven steel piles, the degree of weathering may be ignored. If the "excellent" range in rock strengths is the only description considered for small displacement, driven steel piles, this method would line up almost exactly with the range for Rehnman and Broms (1971).

4.2 LADANYI AND ROY (1971)

As discussed in Chapter 2, Ladanyi and Roy (1971) is a method developed for socketed piles and hence there is some ambiguity in its application to small displacement driven steel piles. For the discussion to follow, the ultimate calculated toe resistance, in unit of force, will be calculated using the net steel area of the pile. For the Ladanyi and Roy (1971) method, the base of the pile, B, is essentially the width of the socket considered. Although the width of a steel pile such as that examined in this thesis may be similar, the actual contact width of a driven small displacement steel pile is likely not as large as these socketed piles (see Figure 12). Since the pile thickness is much smaller than the base of a socketed pile, its stress distribution will have an influence on fewer discontinuities in the rock (see Figure 13). This suggests that discontinuities should have a much smaller effect on the calculation of pile toe resistance if considering the steel pile thickness rather than steel pile base. For this research, the width of the steel pile, B, is referred to as B_1 in Figure 12. For a small displacement steel pile such as an H-pile or open-ended pipe pile, the width of the pile could also be considered as the width of the steel in contact with the rock, shown as B_2 in Figure 12.

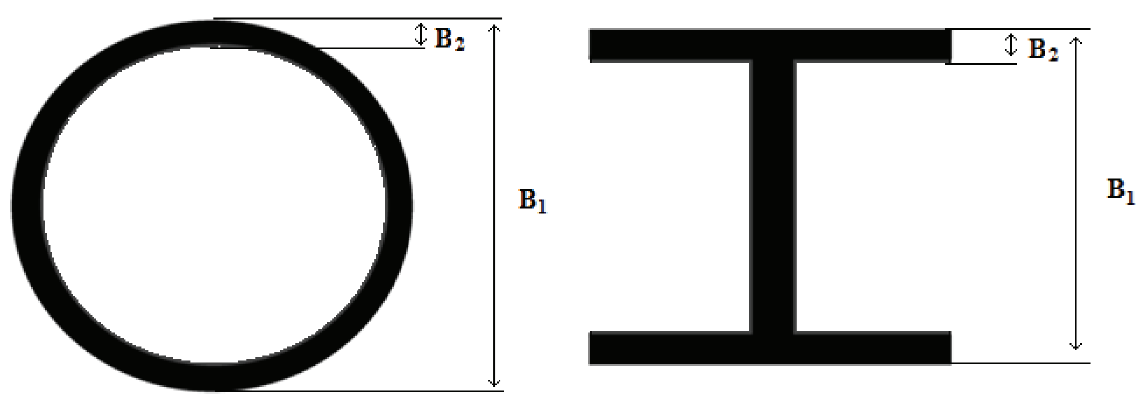

Figure 12 Definition of B_1 and B_2 for small displacement piles examined in this thesis

Table 1, presented in Chapter 2, was developed using equation 19 with typical pile widths, B_1, for sockets (i.e. large pile width). For the given B_2 situation shown above (i.e. small pile width), values of K_{sp} will be much higher than those in Table 1 and hence equation 19 as used in CFEM (2006) was used to determine K_{sp} for this situation. For the cases in this research, equations 21 and 22, developed by Priest and Hudson (1976), were used to estimate spacing of discontinuities from values of RQD in the database. Aperture of discontinuities was lacking from all borehole records and hence a median value of 0.005 (see Figure 1) was assumed for calculations. It is also important to note that when B_2 was used to calculate K_{sp} , the same B_2 was also used to calculate "d" for the sake of consistency. The parameter "d" in equation 18 also remained limited to a value of 3.

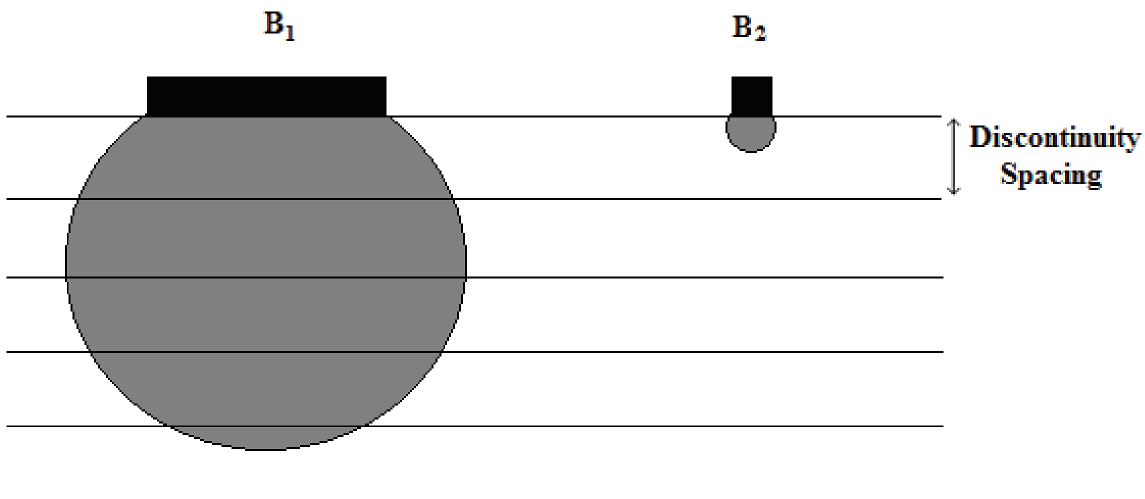

Figure 13 Zone of influence example for B_1 and B_2

Ladanyi and Roy (1971) is somewhat different than the methods discussed in Section 4.1 in that for these previous methods, only the unconfined compressive strength of the rock was required for estimating the ultimate toe capacity of the pile. For Ladanyi and Roy (1971) as described in the CFEM (2006), there are three parameters required to estimate this toe capacity: the unconfined compressive strength, the depth factor (d) and "K_{sp}". Therefore, producing plots similar to those in section 4.1 (i.e. in terms of rock strength versus measured pile toe capacity) was not possible as these three parameters could potentially vary for each data set. To compare the calculated and measured toe resistances, plots were produced with calculated values on the x-axis and measured values on the y-axis. The best fit of the data, with a slope of "η" can be described using the following equation:

[37] $$q_t = \eta q_{tc}$$

Where:

q_{tc} = ultimate calculated toe bearing capacity (F/L^2)

For equation 37, q_t represents the ultimate measured toe bearing capacity, while q_{tc} is its calculated counterpart. Each plot in this section (Figure 14-16) contains a solid line which establishes equality between calculated and measured values (i.e. the 1:1 line). This line is useful to include on the plots as it distinguishes where the calculated ultimate toe capacity exceeds the measured ultimate toe capacity.

4.2.1 Pile Width, B_1

A summary of the pile and rock parameters used (i.e. "q_u", calculated values for discontinuity spacing, "K_{sp}" and "d") for this approach is shown in Table 6. For each pile in this thesis, the discontinuity spacing fell within (or below) the 0.3 to 1m range found in Table 1, which led to a K_{sp} of 0.1. The plot of calculated versus measured pile toe capacity for this method can be seen in Figure 14. A factor of safety of 3 was used to "un-factor" $K_{sp.}$

Table 6 Inputs to Ladanyi and Roy (1971) as per CFEM (2006) using B_1

Number	q_u (MPa)	B_1 (m)	Spacing (m)	K_{sp}	d
1056734	8	0.32	0.033	0.1	1.19
1017681	10	0.40	0.028	0.1	3.00
	10	0.36	0.028	0.1	3.00
121612385	18	0.36	0.033	0.1	3.00
	8.5	0.36	0.031	0.1	3.00
	14.3	0.508	0.033	0.1	2.07
	14.3	0.508	0.033	0.1	1.99
1046136	8	0.31	0.033	0.1	3.00
121613582	16	0.36	0.050	0.1	3.00
121613585	5.4	0.31	0.031	0.1	1.67
121611479	9.9	0.31	0.048	0.1	3.00
	8.1	0.31	0.015	0.1	3.00
7892J	10	0.31	0.033	0.1	1.00
121910608.6	10.8	0.31	0.033	0.1	3.00
121614157	15	0.31	0.027	0.1	1.85

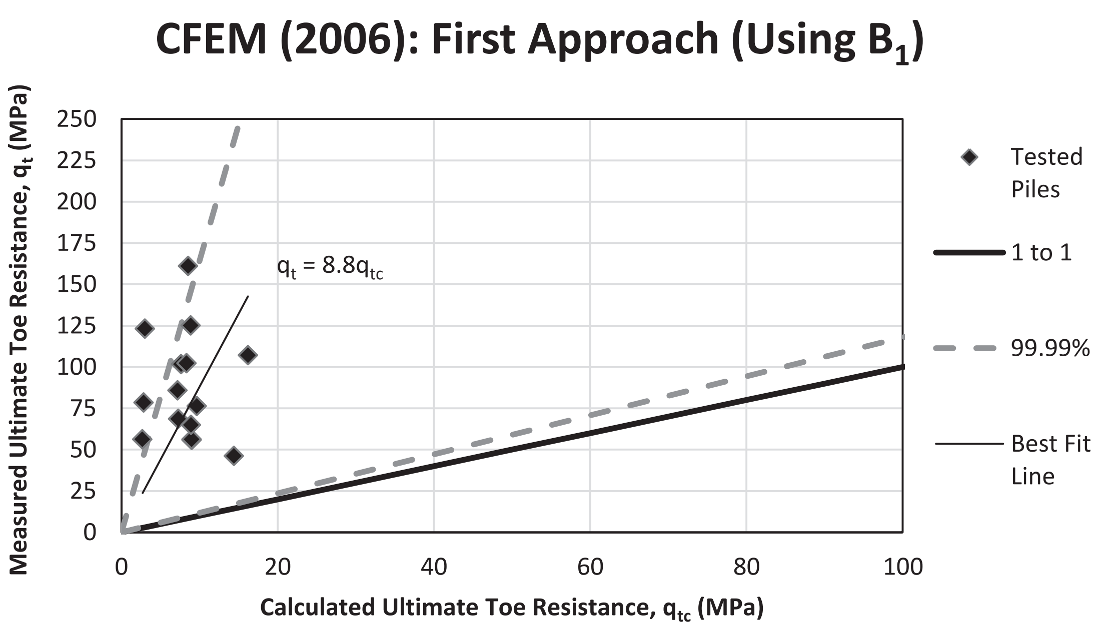

Figure 14 Ladanyi and Roy (1971) as per CFEM (2006), using B_1 approach

As can be seen, in Figure 14, the use of the pile width, B_1, results in very conservative calculations of toe resistance. The best fit line from Figure 14 demonstrates that with this approach, the average measured ultimate toe resistance is 8.8 times larger than the calculated ultimate toe resistance.

4.2.2 Pile Thickness, B_2

When using the pile thickness of B_2, the calculated values for discontinuity spacing, "K_{sp}" and "d" can be seen below in Table 7. Use of the pile thickness B_2 had a significant effect on "d"; all values of "d" reached the maximum limitation except for the one case where the pile toe resided on the surface of the bedrock. This change also had a significant effect on increasing the value of "K_{sp}", as seen in Table 7.

Table 7 Inputs to Ladanyi and Roy (1971) as per CFEM (2006) using reinterpreted B_2

Number	q_u (MPa)	B_2 (m)	Spacing (m)	K_{sp}	d
1056734	8	0.0095	0.033	0.70	3.0
1017681	10	0.0356	0.028	0.30	3.0
	10	0.0156	0.028	0.30	3.0
121612385	18	0.0179	0.033	0.45	3.0
	8.5	0.0179	0.031	0.30	3.0
	14.3	0.0127	0.033	0.57	3.0
	14.3	0.0127	0.033	0.72	3.0
1046136	8	0.0155	0.033	0.52	3.0
121613582	16	0.0179	0.050	0.37	3.0
121613585	5.4	0.0154	0.031	0.32	3.0
121611479	9.9	0.0154	0.048	0.39	3.0
	8.1	0.0154	0.015	0.25	3.0
7892J	10	0.0183	0.033	0.59	1.0
121910608.6	10.8	0.0110	0.033	0.71	3.0
121614157	15	0.0154	0.027	0.30	3.0

The plot of this reinterpreted approach, along with the best fit line of this data set and its 99.99% confidence interval can be seen in Figure 15. Like in the previous section, the upper and lower slopes of these different confidence intervals were determined (for 95%, 98%, 99.9% and 99.99%) and are shown in Table 8.

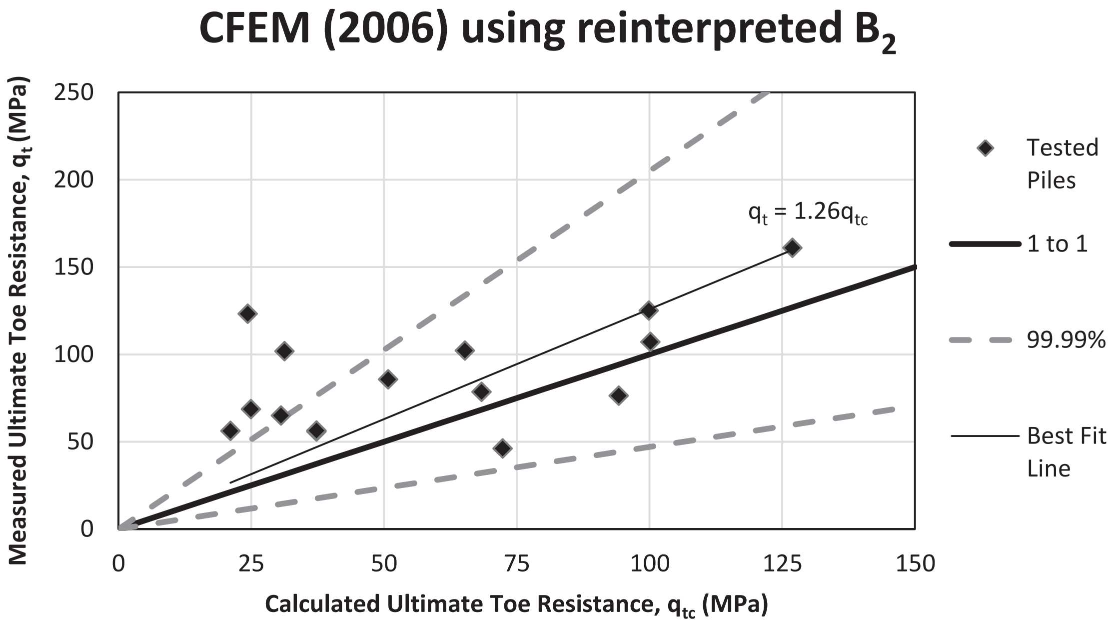

Figure 15 Ladanyi and Roy (1971) as per CFEM (2006) using reinterpreted B_2 approach

Table 8 Ladanyi and Roy (1971) as per CFEM (2006) using reinterpreted B_2 confidence intervals

Interval (%)	Lower Bound	Upper Bound
95	0.94	1.57
98	0.87	1.65
99.9	0.65	1.87
99.99	0.47	2.05

As shown on Figure 15, the reinterpreted approach to using CFEM (2006) for small displacement, driven steel piles is much more effective than that examined in section 4.2.1. This data set provided a "η" value of 1.26. It can be seen that this best fit line is very close to the one to one line, but is still situated on its "conservative" side.

Since the other design methods in section 4.1 were analyzed based only rock strength, it is difficult to compare these results with that of section 4.1. To provide some level of comparison, the best fit developed for the dataset in Section 4.1 was plotted in a similar fashion, in terms of calculated versus measured toe capacities. The resultant confidence interval slopes can be seen in Table 9, while the plot with the best fit and 99.99% confidence interval for the data set can be seen in Figure 16.

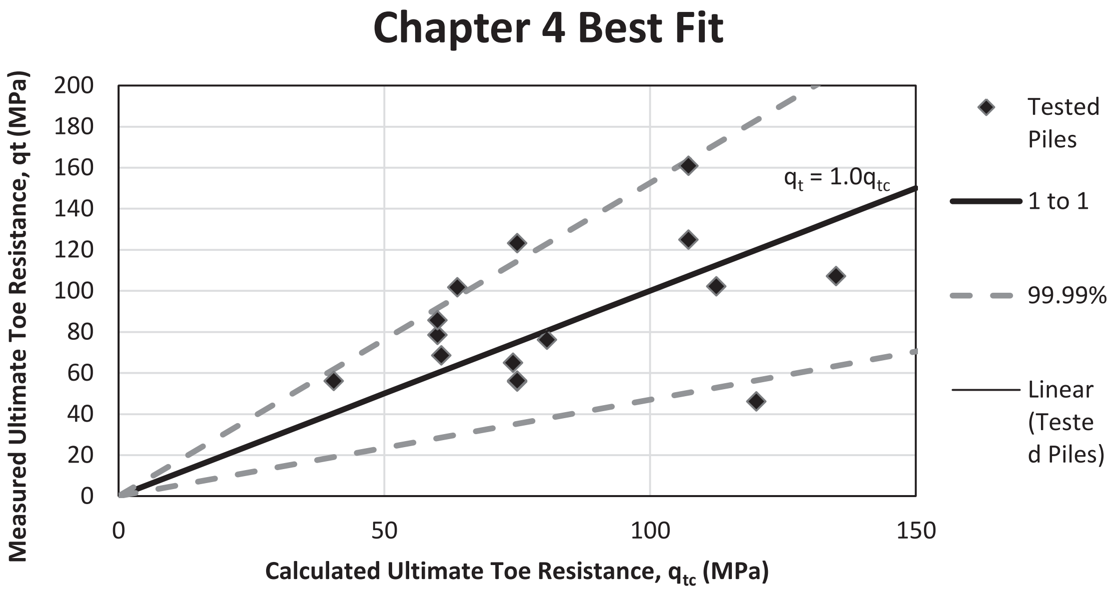

Figure 16 Chapter 4 “best fit” calculated vs. measured

Table 9 Chapter 4 “best fit” confidence intervals using measured vs. calculated

Interval (%)	Lower Bound	Upper Bound
95	0.79	1.21
98	0.74	1.26
99.9	0.59	1.41
99.99	0.47	1.53

Figure 16 shows that considering this best fit approach produces a “η” value of 1.0, which lies exactly on the one to one slope. Comparing Table 8 and Table 9 exhibits that the confidence intervals for the “best fit” approach developed in 4.2.1 provides comparable results to the B_2 approach presented in this section, with CFEM (2006) being slightly more conservative. All work completed in this section can be seen in Appendix C.

4.3 Summary and Conclusions

When plotting the dataset of unconfined compressive strength versus ultimate measured pile toe capacity, the best fit of the data set was found to have a slope “η” of 7.5. The confidence intervals for this best fit line were also determined in order to compare to existing design methodologies. Overall, it was seen that most of the methods developed for drilled sockets were too conservative for the usage with small displacement, steel driven piles. Zhang and Einstein (1998) and Rowe and Armitage (1987) were both proven to be excessively conservative in all cases. Coates (1981) was also found to be too conservative for most cases, except when considering a 99.99% confidence interval. The existing method that exhibited the best predictive ability for driven steel piles was the only empirical method developed for the intentions of being used for driven steel piles, the method that was developed by Rehnman and Broms (1971). It was found that although for some cases using a factor of 6 may be appropriate, a factor of 4 or 5 would be more appropriate when considering more conservative confidence intervals.

By qualitative analysis, it was determined that Hoek and Brown (1980) was also likely too conservative when applied in the same manner as designed for drilled sockets. However, if it is assumed that joint weathering has little effect on the toe resistance of driven steel piles, besides its effect on rock strength, this method lines up well with Rehnman and Broms (1971). Calculating ultimate toe resistances with this method was not possible due to the lack of rock joint aperture sizing from the data.

Ladanyi and Roy (1971) as described in CFEM (2006) using pile width for a base (B_1) was found to not be appropriate for usage with small displacement, driven steel piles. This method was much too conservative in order to be considered a reasonable predictive method. This method was reinterpreted by the author by using the pile thickness (B_2) as the base. The usage of the pile thickness was justified by considering the smaller zone of influence of a small displacement, driven steel pile in comparison to a more massive socketed pile. This factor of B_2 was used in the calculation of "K_{sp}" which led to much larger values of "K_{sp}". It was also used in the calculation of the depth factor, d. The results for this method were found to be very similar to the results of the best fit line developed in Chapter 4; however it was slightly more conservative.

It was determined that both Rehnman and Broms (1971) and the reinterpreted version of CFEM (2006) as developed by Ladanyi and Roy (1971) exhibit the best predictive ability to determine ultimate toe capacity of small displacement, steel driven piles. The one difference is that Rehnman and Broms (1971) is a very simple approach that requires only unconfined compressive strength while Ladanyi and Roy (1971) requires a multitude of different variable parameters, some of which are frequently not determined for geotechnical projects (aperture and spacing of rock joints). Given this, it can be seen that Rehnman and Broms (1971) would be useful for practical applications.

The best fit line of this data set provides a real world sample of data that to the knowledge of the author, previously was not available. Rowe and Armitage (1987) and Zhang and Einstein (1980) had collected field data sets for drilled sockets, but it is believed that before this, no similar data set for small displacement, driven steel piles have been analyzed. While Rehnman and Broms (1971) and Ladanyi and Roy (1971) have both proven to be useful methodologies, both of these empirical methods were developed through smaller scale lab testing. This resultant best fit line should provide engineers with the same estimating tool for small displacement, steel driven piles that Rowe and Armitage (1987) and Zhang and Einstein (1980) provided for drilled sockets.

CHAPTER 5 COMPARING EMPIRICAL RELATIONSHIP TO OTHER DATA SOURCES

In Chapter 4, it was found that the best fit line of the database developed in Chapter 3 had a slope, "η", of 7.5. The slopes of the various confidence intervals ranging from 95% to 99.99% for this best fit line were also presented. This chapter will compare these relationships for toe capacity based on unconfined compressive strength data to data obtained, yet not included in this previous data set. It will also compare these relationships to data from literature. These comparisons will be made in an attempt to verify the effectiveness of the relationships at predicting reasonable ultimate toe capacities of driven small displacement piles, particularly for design applications.

5.1 Stantec Database Cases with Missing Rock Strengths

As discussed in Chapter 3, there were numerous piles not included in the database for various reasons. Many piles were excluded from the database because the geotechnical site investigation for that site did not include the laboratory testing required to distinguish rock strength. Without complete testing, specific rock strengths could not be used for the piles on the correlated site and the data was considered incomplete. Although lacking numerical rock strength values, many of these sites contained detailed rock descriptions that could lead to an estimated value of rock strength. Six of such sites will be discussed in this section. Site details for the ten piles to be discussed from these six sites and their rock descriptions can be found in Table 10.

Table 10 Site details for piles lacking rock strengths

Job Number	Pile	Pile Size	Pile Toe (kN)	Blows/ 25 mm	BOR/ EOID	A_t (m^2)	q_t (MPa)
121612915	A	HP360X152	1685	12	BOR	0.0194	86.9
	B	HP360X152	1731	12	BOR	0.0194	89.2
S2297	C	HP8X36	285	5	BOR	0.0068	41.7
121612336	D	OEPP508x12.7	2884	15	BOR	0.0198	145.9
	E	HP 360X174	2673	10	BOR	0.0222	120.4
1031017	F	OEPP 16X0.5	1569	9	BOR	0.0157	99.9
11558	G	HP310X110	1070	10	BOR	0.0141	75.9
	H	HP310X110	2161	6	BOR	0.0141	153.3
	I	HP310X110	1601	5	BOR	0.0141	113.5
121614157	J	HP310X110	1528	10	BOR	0.0141	108.4

Job Number	Rock Description
121612915	Severely fractured to fractured, slightly weathered, fine grained sandstone.
S2297	Highly weathered grey to brown, very weak to weak, closely jointed mudstone.
121612336	Very poor to fair quality brown siltstone. Highly weathered.
1031017	Highly to completely weathered, very soft to soft granite. (Near soil-like)
11558	Fine grained sandstone bedrock (G). Weathered sandstone (H,I)
121614157	Very poor to fair brown mudstone (J)

As can be seen, nine of these piles are bearing on sedimentary rock that can be classified as “very weak” or with “very low” rock strength. The other pile (pile F from site 1031017) is on a near soil like granite formation. Using the guidelines in the Stantec Consulting Limited geotechnical site investigation reports, this description implies a rock strength between 1 MPa and 25 MPa for these sites. Table 10 shows that these piles contain all other constraints designated in Chapter 3 to be a requirement to be considered “good” data.

In this analysis the expected value of unconfined compressive strength for each pile was determined by dividing the known measured pile toe capacity by the best fit of 7.5. These expected rock strengths, along with the upper and lower 99.99% confidence interval for each of these piles represented by an error bars, can be seen in Figure 17. In Figure 17, the range of 1 to 25 MPa is represented by bolded lines. The calculated ranges of the accepted rock strengths for each pile as designated by the 99.99% confidence intervals are displayed in Table 11.

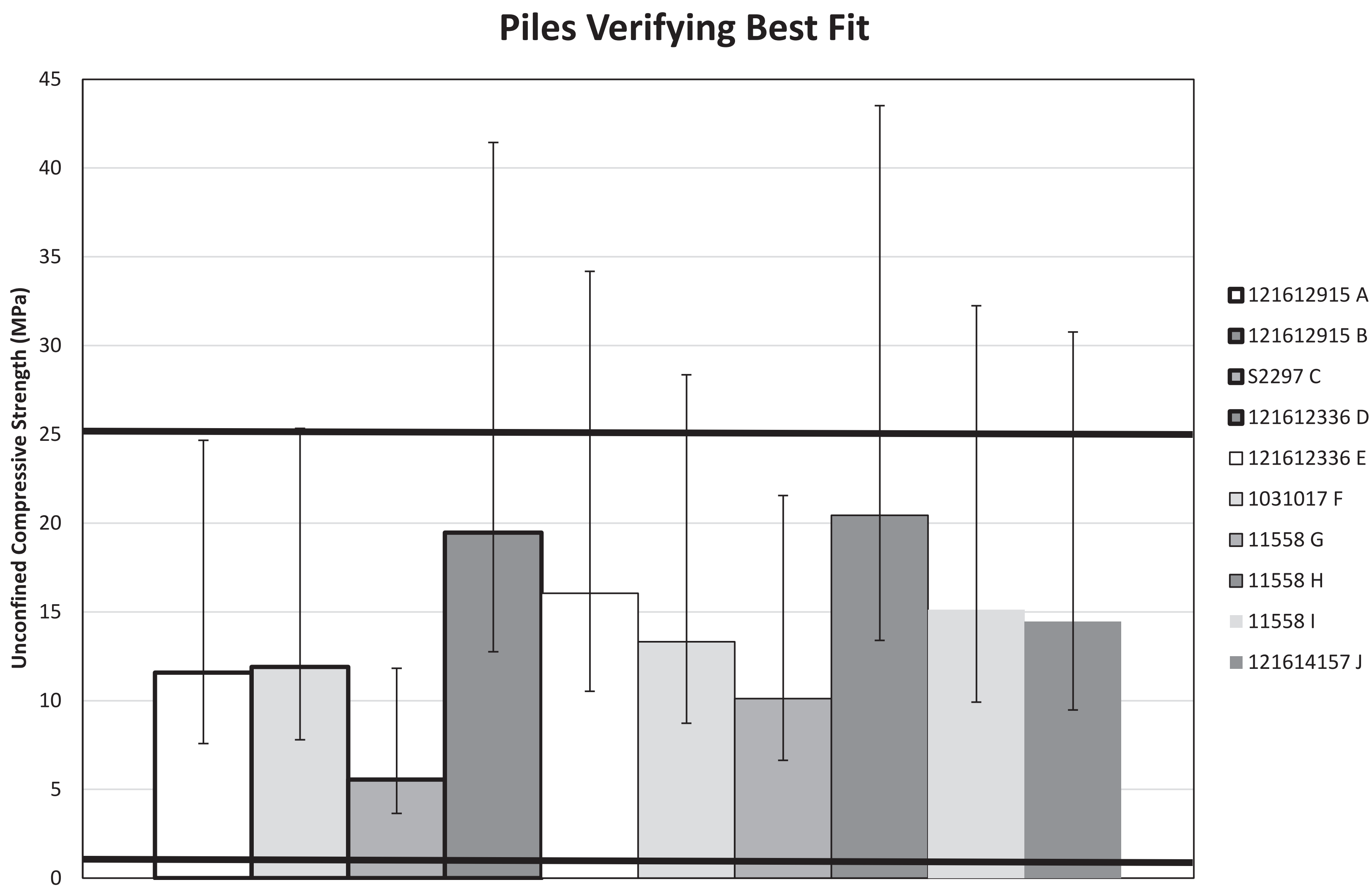

Figure 17 Analyzing expecting rock strengths using best fit method

Table 11 Ranges of rock strengths for piles verifying best fit

		Rock Strengths (MPa)		
Job Number	**q_t (MPa)**	**-99.99%**	**Best Fit**	**99.99%**
121612915	86.9	24.7	11.6	7.6
	89.2	25.3	11.9	7.8
S2297	41.7	11.8	5.6	3.6
121612336	145.9	41.4	19.5	12.8
	120.4	34.2	16.1	10.5
1031017	99.9	28.4	13.3	8.7
11558	75.9	21.5	10.1	6.6
	153.3	43.5	20.4	13.4
	113.5	32.2	15.1	9.9
121614157	108.4	30.8	14.4	9.5

As can be seen in Figure 17, the majority of these piles fit this best fit range of 1 to 25 MPa extremely well. The best fit for all of these piles are between 5.6 MPa and 20.4 MPa, with most of them landing near the exact middle of the 1 MPa to 25 MPa range. The majority of the error bars for these piles also remain mostly in the 1 MPa to 25 MPa range. The 99.99% confidence interval error bars of six of these piles extend partially out of this expected rock strength range, and only two of them (121612336 D and 11558 H) extend out of this range to any considerable degree. Overall, all of these piles appear to fit in very well with the previously established best fit line and its confidence interval range.

5.2 Using Matsumoto et. al. (1995)

Another way to evaluate the best fit range developed in Chapter 4 is to use data found from other sources in literature. A search was made through literature for piles with data sets that were considered "complete" (as designated in Chapter 3). It was discovered that piles in literature with "complete" data sets were extremely rare. Most piles in literature provide little more than the rock type, and very few give so much as a detailed rock description. Overall, only one pile, that which was found in Matsumoto et. al. (1995) provided an unconfined compressive strength.

Matsumoto et. al. (1995) examines the use of multiple steel driven piles on an extremely soft mudstone. One pile, pile T_1, contained adjacent cone penetration tests results to describe the rock available on site. This pile had a base area of 0.041 m^2 and was found to have an ultimate toe resistance of 500 kN by static load testing. An unconfined compressive strength test was completed (0.8 MPa), however it is unclear as to what depth that this rock was found. The completed cone penetration test results allowed the author to estimate the unconfined compressive strength through calculation and to compare the result to this existing value. At the base of pile T_1, the measured cone tip resistance (q_c) was about 3.2 MPa, while the measured pore water pressure between the piezocone tip (u_{bt}) was about 1.35 MPa. With this known information, the corrected cone tip resistance as described by Lunne et. al. (1997) can be calculated as follows:

[38] $$q_{TC} = q_c + (1 - a)u_{bt}$$

Where:
q_{TC} = corrected cone tip resistance (F/L^2)
q_c = cone tip resistance (F/L^2)
a = net area ratio (for cone penetrometer test)
u_{bt} = pore water pressure behind piezometer tip (F/L^2)

For this equation, the value of "a" is described in Lunne et. al. (1997) to range from 0.55 to 0.9. For this calculation, a value of 0.6 was assumed, as typical values are usually around the lower end of this range. The unconfined compressive strength, q_u, is twice the undrained shear strength. Kulhawy and Mayne (1990) describes the empirical relationship used to determine the undrained shear strength from cone penetrometer testing:

[39] $$c_u = \frac{q_{TC} - \sigma_{vo}}{N_k}$$

Where:
c_u = undrained shear stress (F/L^2)
σ_{vo} = overburden stress (F/L^2)
N_k = cone bearing factor

The cone bearing factor, N_k, is typically decided empirically by calibration of the cone. Since this was not possible, the typical value of 9 found in Kulhawy and Mayne (1990) was used. The overburden stress was estimated to be 144 kN/m^2 using 8 m of soil and rock with an estimated unit weight of 18 kN/m^3 (Coduto, 1999). Overall, this lead to an undrained shear strength of 0.8 MPa, which in turn is exactly the same as that measured with the unconfined compressive strength test.

As seen in Figure 19, by comparing this unconfined compressive rock strength to the measured ultimate toe resistance, the best fit range determined in Chapter 4 could be evaluated. The empirically estimated capacity was found to be very conservative because the measured ultimate pile toe capacity greatly surpasses the calculated ultimate pile capacity. In this case, this was not surprising as the rock strength was low enough that it could actually be considered a soil.

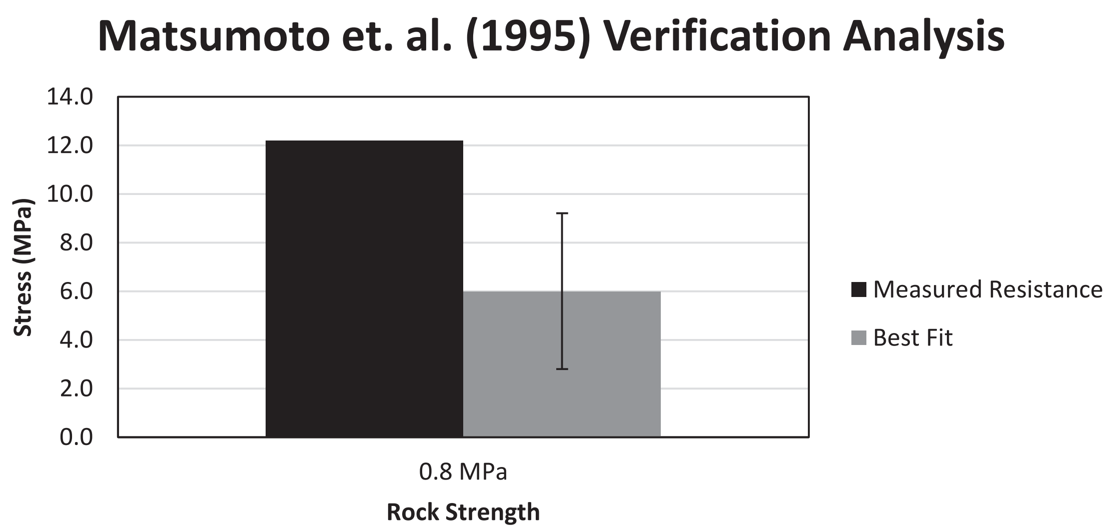

Figure 18 Verification of best fit range using Matsumoto et. al. (1995)

5.3 Summary and Conclusions

In this chapter, an attempt was made to verify the best fit relationship (and range) that was developed in Chapter 4. Data that was excluded from the data set because of missing rock strengths was used to evaluate this method. A range of estimated rock strengths determined from the rock descriptions were used for each pile as a means of evaluating this relationship. It was found that this relationship would work well from a design perspective. A pile case from the literature (Matsumoto, 1995) was also used in attempt to verify this range. This attempt was not as successful, likely due to the extremely weak nature of the rock for this site.

CHAPTER 6 SUMMARY AND CONCLUSIONS

6.1 SUMMARY AND CONCLUSIONS

Small displacement driven steel piles are a very useful type of deep foundation for construction sites containing dense granular overburden soils and shallow bedrock because of the durable nature of steel and the ability to drive the small displacement piles through these soils conditions, to the rock. Although this is a very practical construction method when considering a pile bearing on rock, design codes typically ignore this topic or simply suggest using engineering judgment and/or local experience. The purpose of this thesis was to propose the most appropriate and accurate method of estimating ultimate toe capacity of small displacement driven steel piles by reviewing known methods. It was hypothesized that the toe capacity could be adequately predicted with some level of reliability through the knowledge of geotechnical site information, including rock strength and depth and “complete” pile details.

In Chapter 2, a collection of empirical and theoretical methods for determining pile toe capacity on rock was compiled. The formation and basis of each of these methods was described in detail. Only one method developed specifically for small displacement driven steel piles was found; that developed by Rehnman and Broms (1971). A collection of methodologies for socketed pile toe capacity on rock was also included in this review. It was believed by the author that these methods would likely be more conservative than Rehnman and Broms (1971) because the toe resistance of socketed piles is affected greater by rock discontinuities. The drilled socket theories included in this thesis consist of methods by Bell (1915), Coates (1981), Rowe and Armitage (1987), Zhang and Einstein (1998), Ladanyi and Roy (1971) and Hoek and Brown (1980). However, it was explained that if the effect of weathering on ultimate toe resistance for driven steel piles is minimal, Hoek and Brown (1980) is very comparable to Rehnman and Broms (1971).

The process for a data collection method was outlined. For this thesis, only optimum, or “complete”, data points were included in the database. Only small displacement, driven steel piles driven to rock were considered. It was decided that piles enduring a maximum of 15 hammer blows per 25 mm of driving would be permitted in the inclusion in this database to ensure full pile mobilization. All piles were also required to have a measure pile toe resistance determined through re-strike conditions and have a listed pile toe elevation. It was deemed necessary for the geotechnical site investigation for each pile to include an unconfined compressive strength, RQD, rock profile and rock elevations. Detailed mapping for both boreholes and pile locations were required for each site. Hammer energy and rock core recovery were also considered in the process. The final database contained 15 piles from 10 different construction sites. The parameters for each of these sites were presented in Chapter 4.

When considering the database in Chapter 3, a best fit line of the database comparing ultimate measured pile toe capacity to unconfined compressive strength rock for small displacement driven steel piles was plotted. It was found that this relationship produced a best fit line of $7.5q_u$. Confidence intervals of 95%, 98%, 99.9% and 99.99% were also determined for this best fit line using regression analysis. This collection of data and the suggested design approach (i.e. best fit line), to the knowledge of the author, is the first of its kind for small displacement driven steel piles on rock.

This best fit line and its confidence intervals were used to analyze the effectiveness of the empirical and theoretical methods collected in Chapter 2. Section 4.1 inspected the methods that could directly relate ultimate pile toe capacity and unconfined compressive strength. It was found that Zhang and Einstein (1998) and Rowe and Armitage (1987) were very conservative. Coates (1981) also proved to be too conservative as well except when considering the 99.99% confidence interval of the best fit line. It was not surprising that these methods proved to be conservative when applied to small displacement, driven steel piles because they are all methods designed for drilled sockets. The existing linear method found to best exemplify this best fit relationship was that by Rehnman and Broms (1971). This was as expected because it was the only method examined with the intended purpose of being used for small displacement driven steel piles. It was found that using a factor between 4 and 5 with Rehnman and Broms (1971) was most effective when taking the confidence intervals of the best fit line into consideration.

Section 4.2 analyzed the method suggested by Ladanyi and Roy (1971) as displayed in CFEM (2006). This section investigated two approaches to this method; the use of the pile width (B_1) for the pile base and a reinterpreted approach of using the pile thickness (B_2) for the pile base. The justification of the reinterpreted method is based on the effect that the small displacement pile will have on rock discontinuities when compared to a larger drilled socket, for which the equation was originally intended. It was found that using B_1 led to this method being over eight times too conservative. Using CFEM (2006) with B_2 proved to be more accurate. This method was determined to only be about 1.25 times too conservative in comparison with the best fit line developed in Section 4.1.

Overall, it was found that the two most effective existing methods of estimating ultimate pile toe resistance of small displacement driven steel piles were Rehnman and Broms (1971) and the reinterpreted application of Ladanyi and Roy (1971) as described in CFEM (2006). The difference between these two methods is that Rehnman and Broms (1971) requires only one parameter, the unconfined compressive strength, and thus is quicker and more efficient to use.

In Chapter 5, the best fit line of $7.5q_u$ developed in Chapter 4 was evaluated using data from other sources. Ten piles obtained from the records of Stantec Consultants Inc. were considered. These piles contained geotechnical site investigations without rock strengths; however, detailed rock descriptions were present in these reports. Using an estimated range of rock strengths determined from the rock description, the best fit line was evaluated and determined to be appropriate for these piles. A pile from Matsumoto et. al. (1995) was also used to evaluate this best fit. This pile was found to not conform to the best fit line, possible because of the particularly weak nature of the rock profile on this site.

6.2 Recommendations For Future Work

The results produced in this thesis are promising, but are based on a collection of only 15 piles. Compiling a larger database of piles could help refine the best fit line developed in this thesis and to shrink the range of the confidence intervals for this data set. It would be even more beneficial if the additions to this database included a wide range rock types from different locations in addition to the piles collected from Atlantic Canada.

It is also recommended that the theory for Ladanyi and Roy (1971) be expanded for the usage with driven steel piles. It was demonstrated in Chapter 4 that there is a strong relationship using this method when considering the reinterpreted base size (B_2) suggested by the author. It would be very beneficial to engineers if this reinterpreted application could be proven theoretically. It would also be a good idea for the theory of the depth of embedment with Ladanyi and Roy (1971) to be re-examined. It was found that when using the reinterpreted depth size (B_2) that this value reached its maximum very easily since the thickness is very thin in comparison to the depth of embedment. It should be noted that the work completed in this thesis was based solely on the ultimate toe capacity driven of small displacement steel driven piles. In no way was the estimation of pile settlement taken into consideration. Although it is expected that settlement of piles bearing on rock is not likely to be a major issue, it is recommended that this aspect be investigated.

BIBLIOGRAPHY

ASTM Standard D7012-10 (2010). Standard Test Method for Compressive Strength and Elastic Moduli of Intact Core Specimens under Varying States of Stress and Temperatures. ASTM International, West Conshohocken, PA. Retrieved from ASTM Digital Library.

ASTM Standard D5731-08 (2008). Standard Test Method for Determination of Point Load Strength Index of Rock and Application to Rock Strength Classifications. ASTM International, West Conshohocken, PA. Retrieved from ASTM Digital Library.

Axelsson, G (2002). A conceptual model of pile set-up for driven piles in non-cohesive soil. Geotechnical Special Publication, 116: pp 64-79.

Bell, A.L. (1915). The lateral pressure and resistance of clay, and the supporting power of clay foundations. A Century in Soil Mechanics, ICE, London. pp 93-134.

Carter, J.P. and Kulhawy, F.H. (1988). Analysis and Design of Drilled Shaft Foundations Socketed into Rock. Report No. EL-5918, Empire State Electric Energy Research Corporation and Electric Power Research Institute, New York, NY.

CFEM, (2006). Canadian Foundation Engineering Manual: 4th Edition. Canadian Geotechnical Society, Altona, MB.

Coates, D.F. (1981). Rock Mechanics Principles (Revised, 1981). Canadian Department Mines, Monograph 874.

Coduto, D.P. (1999). Geotechnical Engineering: Principles and Practices. Prentice-Hall, Inc. Upper Saddle River, NJ. 759 p.

Coduto, D.P. (2001). Foundation Engineering: Principles and Practices Second Edition. Prentice-Hall, Inc., Upper Saddle River, NJ. 883 p.

Davisson, M.T. (1973). High capacity piles. Proceedings, lecture series, Innovations in Foundation Construction, ASCE, Illinois Section, 52 p.

Deere, D.U. (1963). Technical description of rock cores for engineering purposes. Rock Mechanics and Engineering Geology, **1**(1): pp. 16-22.

Deere, D.U. and Deere, D.W. (1988). The rock quality designation (RQD) index in practice. ASTM STP 984. Rock Classification Systems for Engineering Purposes, Louis Ed., American Society for Testing and Materials, pp 91-101.

Fellenius, B.H. (1980). The analysis of results from routine pile load tests. Ground Engineering, London, **13**(6): pp. 19-31.

Fellenius, B.H. (2011). Basic Foundation Design, a textbook. Revised Electronic Edition, [www.Fellenius.net], 374 p.

FHWA, Federal Highway Administration (1998). Design and construction of driven pile foundations. Federal Highway Administration, US Department of Transportation, FWDA HI-97-013.

FHWA, Federal Highway Administration (2006). Design and Construction of Driven Pile Foundations– Lessons Learned on the Central Artery/Tunnel Project. FHWA-HRT-05-159.

Glos, G.H., III and Briggs, O.H., Jr. (1983). Rock sockets in soft rock. ASCE Journal of Geotechnical Engineering, **109**(4): pp 758-772.

Hannigan, P.J. (1990). Dynamic monitoring and analysis of pile foundation installations. Deep Foundations Institute, Sparta, New Jersey, p. 69.

Hoek, E. and Brown, E.T. (1980). Underground Excavations in Rock. The Institute of Mining and Metallurgy, London, England. 527 p.

Hovarth, R.G., Kenney, T.C. and Kozicki, P. (1983). Methods of improving the performance of drilled piers in weak rock. Canadian Geotechnical Journal, **20**(4): pp. 525-535.

Kulhawy, F.H. and Mayne, P.W. (1990). Manual on estimating soil properties for foundation design. Report EI-6800, Electrical Power Research Institute, Palo Alta, California.

Ladanyi, B. and Roy, A. (1971). Some aspects of bearing capacity of rock mass. *In* 7th Canadian Symposium on Rock Mechanics, Edmonton. pp 160-190.

Legget, R.F. (1976). Glacial Till: An Inter-disciplinary Study. Royal Society of Canada in co-operation with the National Research Council of Canada, Toronto, ON. 412 p.

Lewis, C.F., Taylor, B.B., Stea, R.R., Fader, G.B.J., Horne, R.J., MacNeill, S.G. and Moore, J.G. (1998). Earth sciences and engineering: Urban development in the metropolitan Halifax area. *In* Karrow, P.F. and White, O.L., Urban Geology of Canadian Cities. Geological Association of Canada. St John's, NFLD. pp 406-444.

Likins, Garland (2011). Personal communication with Garland Likins.

Long, J.H., Maniaci, M. and Samara, E.A. (2002). Measured and predicted capacity of H-Piles. Geotechnical Special Publication, (116): pp 542-558.

Lunne, T., Robertson, P.K., and Powell, J.J.M. (1997). Cone Penetration Testing in Geotechnical Practice. E & FN Spon, New York, NY. 312 p.

MacNeill, Greg (2010-2012). Personal contact with Greg MacNeill.

Matsumoto, T., Michi, Y. and Hirano, T. (1995). Performance of axially loaded steel pipe piles driven in soft rock. Journal of Geotechnical Engineering, **121**(4): pp. 305-315.

Mendenhall, W. and Sincich, T. (1996). A Second Course in Statistics: Regression Analysis Fifth Edition. Prentice-Hall, Inc., Upper Saddle River, New Jersey. pp 154-159.

Meyerhof, G.G. (1951). The ultimate bearing capacity of foundations. Geotechnique, **2**: pp 301-332.

Meyerhof, G.G. (1963). Some recent research on the bearing capacity of foundations. Canadian Geotechnical Journal, **1**(1): pp. 16-26.

Morgano, C.M., White, B.A. (2004). Identifying soil relaxation from dynamic testing. Proceedings of the Seventh International Conference on the Application of Stresswave Theory to Piles 200,. Petaling Jaya, Selangor, Malaysia. pp 415-421.

O'Neill, M. W., Reese, L. C. (1999). Drilled Shafts: Construction Procedures and Design Methods. Report No. FHWA-IF-99-025, Federal Highway Administration.

Pells, P.J.N and Turner, R.M. (1978). Theoretical and model studies relating to footings and piles on rock. Report No. R314, University of Sydney.

Pile Dynamics, Inc. (2000). Case Pile Wave Analysis Program for Windows Manual 2000. Pile Dynamics, Inc., Cleveland, Ohio.

Pile Dynamics, Inc. (2004). Pile Driving Analyzer Manual, PDA--W. January 2004. Pile Dynamics, Inc., Cleveland, Ohio.

Priest, S.D. and Hudson, J.A. (1976). Discontinuity spacing in rock. International Journal of Rock Mechanics and Mining Sciences **13**(5): pp 135-148.

Randolph, M. and Gourvenec, S. (2011). Offshore Geotechnical Engineering. Spon Press, 270 Madison Avenue, New York, NY. 528 p.

Rausche, F., Goble, G. G., Likins, G. E. (1985). Dynamic determination of pile capacity. ASCE Journal of Geotechnical Engineering, **111**(3): pp 367-383.

Rehnman, S.E. and Broms, B.B. (1971). Bearing capacity of piles driven into rock. Canadian Geotechnical Journal, **8**(2): pp 151-162.

Rowe, R.K. and Armitage, H.H. (1987). A design method for drilled piers in soft rock. Canadian Geotechnical Journal, **24**: pp 126-142.

Smith, E.A.L. (1962). Pile driving analysis by wave equation. ASCE Transactions, **127**(1) : pp 425-447.

Terzaghi, K. (1943). Theoretical Soil Mechanics. John Wiley and Sons, Inc., New York, NY.

Whitaker, T. (1976). The Design of Piled Foundations: Second Edition. Pergamon of Canada, Ltd. Queen's Quay West, Toronto, ON. 218 p.

Williams, A.F. (1980). The design and performance of piles socketed into weak rock. Ph.D. thesis, Monash University, Melbourne Australia.

Zhang, L., and Einstein, H.H. (1998). End bearing capacity of drilled shafts in rock. Journal of Geotechnical and Geoenvironmental Engineering, **124**(7): pp. 574-584.

APPENDIX A: PDA/CAPWAP

LimiPile Driving Analyzer ®

121614157

Pile 2 BOR

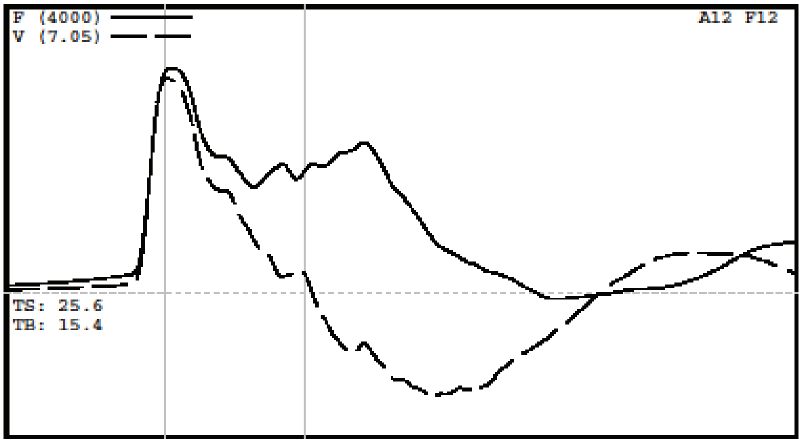

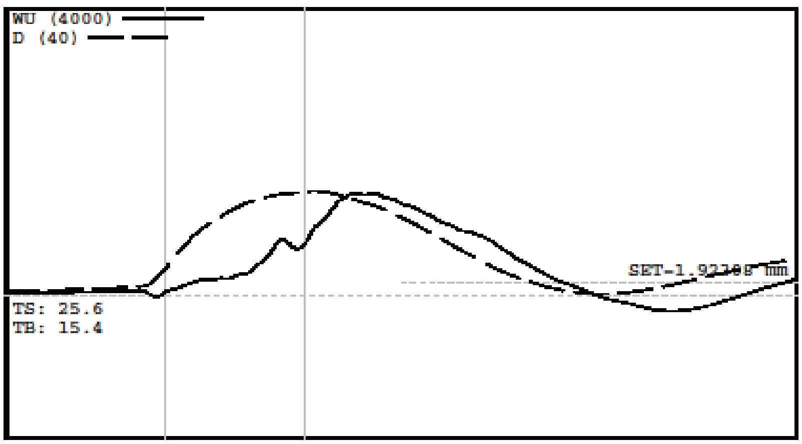

Project Information

PROJECT: 121614157
PILE NAME: Pile 2 BOR
DESCR: West Abutment
OPERATOR:
FILE: Pile 2 BOR.W01
1/26/2012 3:23:38 PM
Blow Number 5

Pile Properties

LE	11.6	m
AR	140.60	cm^2
EM	206843	MPa
SP	77.3	kN/m3
WS	5123.0	m/s
EA/C	568	kN-s/m
2L/C	4.50	ms
JC	1.00	[]
LP	9.9	m

Quantity Results

CSX	222.3	MPa
CSI	225.3	MPa
CSB	119.8	MPa
BPM	37.8	bpm
EMX	31.5	kN-m
RMX	2831	kN
RX7	2913	kN
RX9	2857	kN
WU2	721	kN

Sensors

F1: [5928] 94.3 (1.025)
F2: [8397] 93.8 (1.025)
A1: [6375] 1200 g's/v (0.975)
A2: [6327] 1135 g's/v (0.975)
CLIP: OK
F1/F2: OK 0.99
V1/V2: OK 0.97

Version 2005.096.007

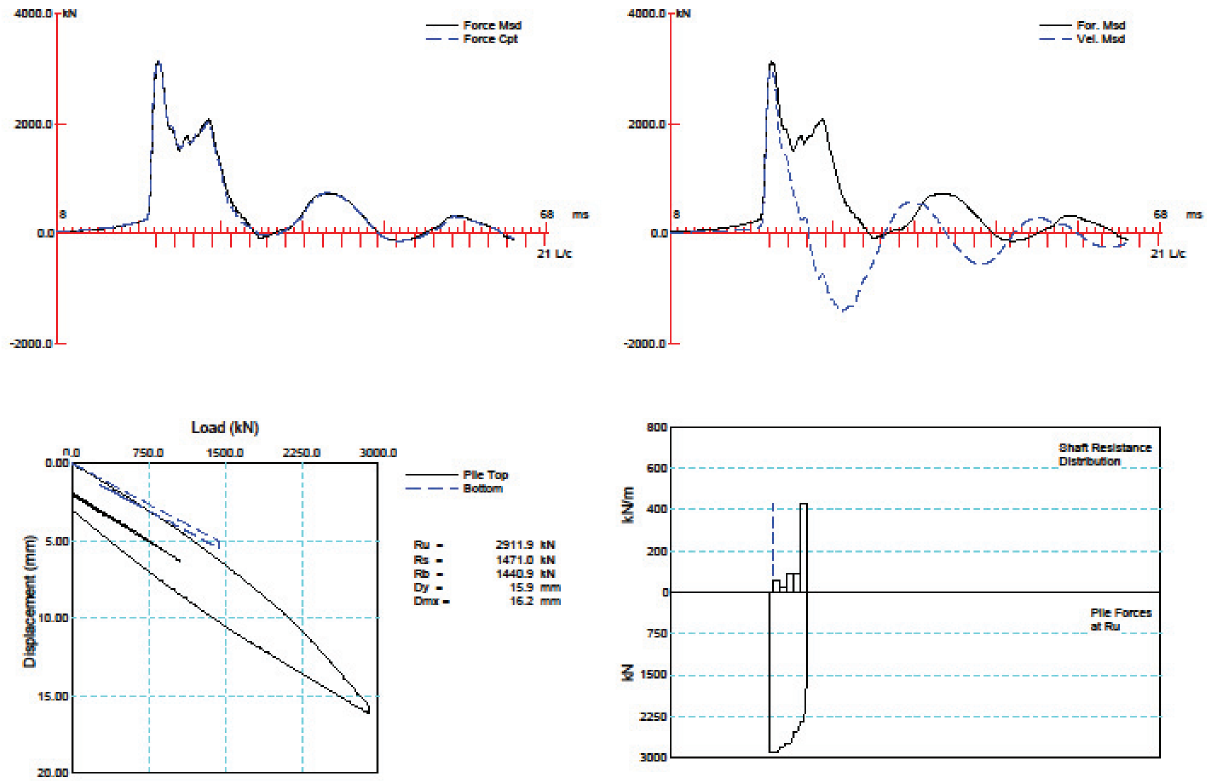
4000.0 kN
2000.0
0.0
-2000.0
8
68 ms
21 L/c
Force Msd
Force Cpt
For. Msd
Vel. Msd
Load (kN)
0.0
750.0
1500.0
2250.0
3000.0
Displacement (mm)
0.00
5.00
10.00
15.00
20.00
Pile Top
Bottom
Ru = 2911.9 kN
Rs = 1471.0 kN
Rb = 1440.9 kN
Dy = 15.9 mm
Dmx = 16.2 mm
800
600
400
200
0
750
1500
2250
3000
kN/m
kN
Shaft Resistance Distribution
Pile Forces at Ru

LimiPile Driving Analyzer ®

121612385

Pile 9 BOR - North Abutment

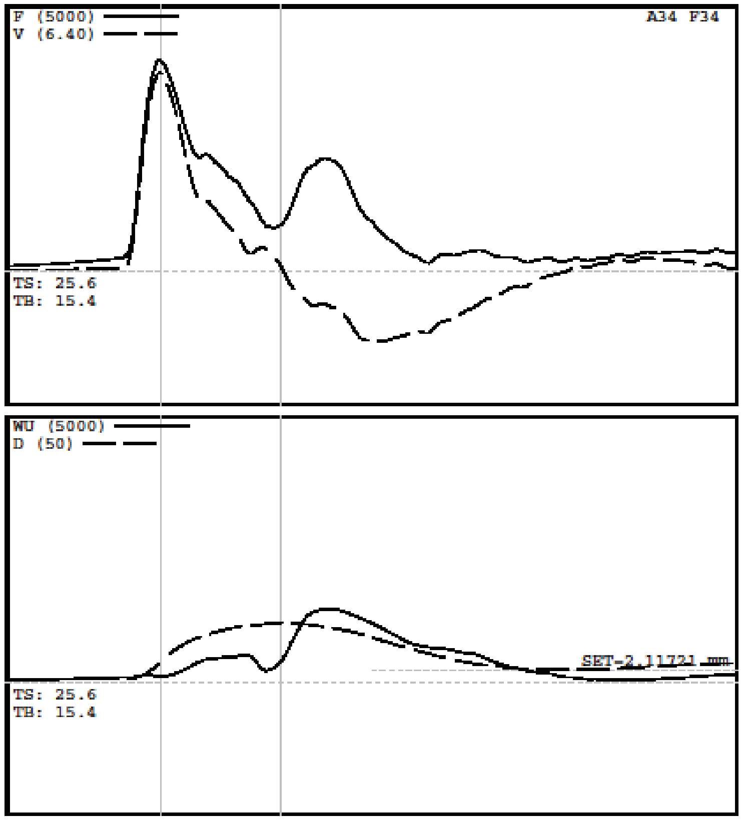

Project Information
PROJECT: 121612385
PILE NAME: Pile 9 BOR - North Abutment
DESCR:
OPERATOR:
FILE: Pile 9 BOR.W01
8/26/2010 4:38:19 PM
Blow Number 5/4

Pile Properties

LE	11.0 m
AR	193.50 cm^2
EM	206843 MPa
SP	77.3 kN/m3
WS	5123.0 m/s
EA/C	781 kN-s/m
2L/C	4.20 ms
JC	1.00 []
LP	10.7 m

Quantity Results

CSX	205.3 MPa
CSI	211.2 MPa
CSB	163.1 MPa
BPM	38.0 bpm
EMX	29.5 kN-m
RMX	2752 kN
RX7	2858 kN
RX9	2784 kN
WU2	371 kN

Sensors
F3: [4169] 97 (0.99)
F4: [8397] 93.8 (0.99)
A3: [257] 370 mv/5000g's (1.01)
A4: [235] 360 mv/5000g's (1.01)
CLIP: OK
F3/F4: OK 0.94
V3/V4: OK 1.03

Version 2005.096.007

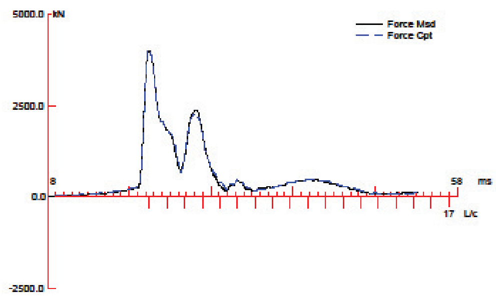
5000.0 kN
2500.0
0.0
-2500.0
Force Msd
Force Cpt
8
58 ms
17 L/c

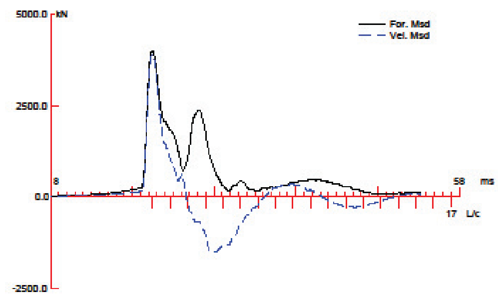
5000.0 kN
2500.0
0.0
-2500.0
For. Msd
Vel. Msd
8
58 ms
17 L/c

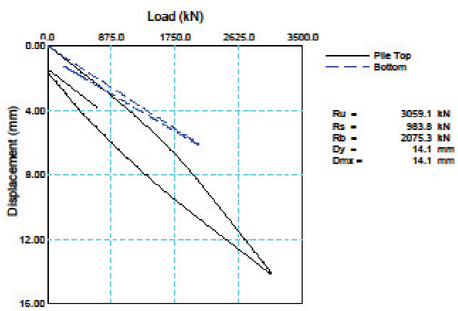
Load (kN)
0.0
875.0
1750.0
2625.0
3500.0
Displacement (mm)
0.00
4.00
8.00
12.00
16.00
Pile Top
Bottom
Ru = 3059.1 kN
Rs = 983.8 kN
Rb = 2075.3 kN
Dy = 14.1 mm
Dmx = 14.1 mm

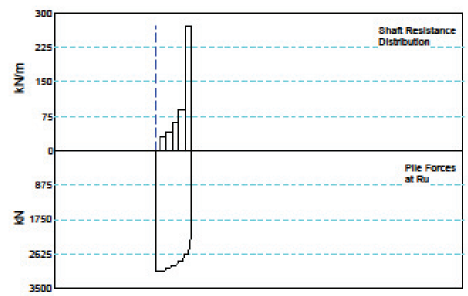
300
225
150
75
0
kN/m
Shaft Resistance Distribution
875
1750
2625
3500
kN
Pile Forces at Ru

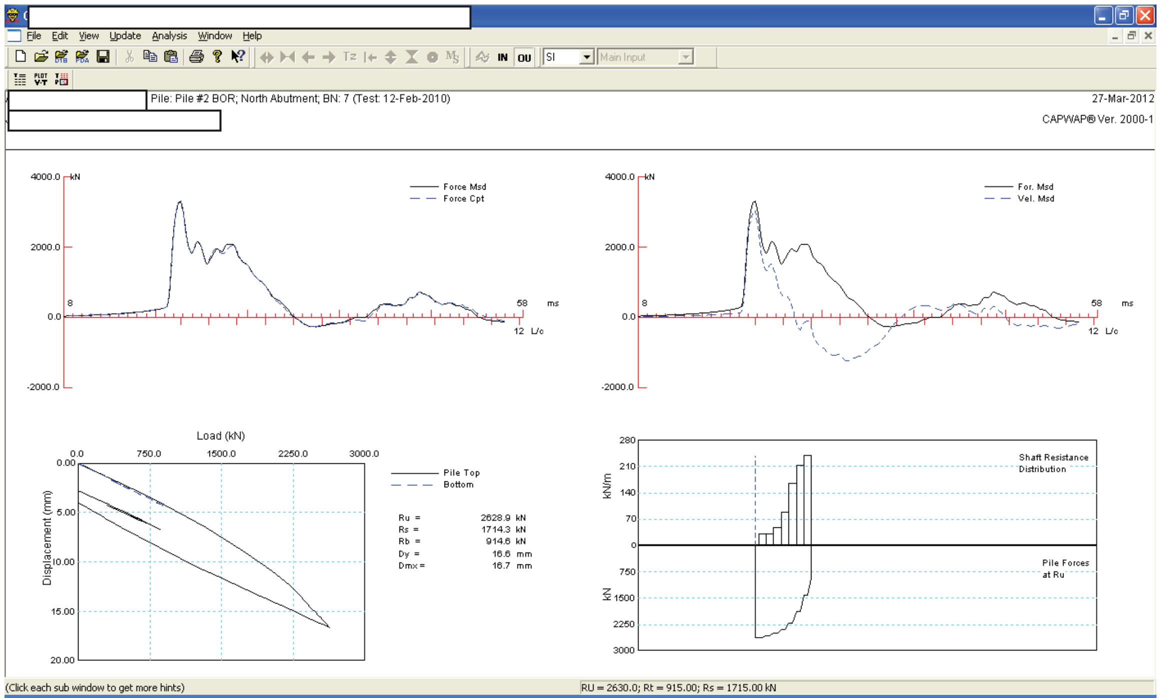
File Edit View Update Analysis Window Help
Pile: Pile #2 BOR; North Abutment; BN: 7 (Test: 12-Feb-2010)
27-Mar-2012
CAPWAP® Ver. 2000-1
Force Msd
Force Cpt
For. Msd
Vel. Msd
4000.0 kN
2000.0
0.0
-2000.0
8
58 ms
12 L/c
Load (kN)
0.0
750.0
1500.0
2250.0
3000.0
Displacement (mm)
0.00
5.00
10.00
15.00
20.00
Pile Top
Bottom
Ru = 2628.9 kN
Rs = 1714.3 kN
Rb = 914.6 kN
Dy = 16.6 mm
Dmx = 16.7 mm
Shaft Resistance Distribution
kN/m
280
210
140
70
0
750
1500
2250
3000
kN
Pile Forces at Ru
(Click each sub window to get more hints)
RU = 2630.0; Rt = 915.00; Rs = 1715.00 kN

APPENDIX B: JOB CHECKLIST AND DATA

APPENDIX: B

Title: Site Selection Criteria Checklist

	Pile Type and Conditions		PDA Report				
Project	**Pile Type/Size**	**In rock**	**Measured Toe**	**Toe Elevation**	**Pile Map**	**BOR**	**Blows/25 mm**
1032593.01	✓	✓	✓	✗	✗	•	✓
1056734	✓	✓	✓	✓	✓	•	✓
1017681	✓	✓	✓	✓	✓	•	•
1020025	✓	✓	✓	✗	✗	•	✗
1038917	✓	✓	✓	✗	✗	•	✗
121612336	✓	✓	✓	•	•	•	•
1021554	✓	•	✓	✓	✓	•	✓
S2297	✓	✓	✓	✗	✓	•	•
121612385	✓	✓	✓	✓	✓	•	•
1046136	✓	✓	✓	✓	✓	•	✓
1049291	✓	•	✓	✓	✓	•	✗
1049353	✓	✓	✓	✗	✓	✓	•
121613582	✓	✓	✓	✓	✓	✓	•
121613585	✓	✓	✓	✓	✓	✓	✓
121611479	✓	✓	✓	✓	✓	✓	✓
7892J	✓	✓	✓	✓	✓	✓	•
1031017	✓	✓	✓	✓	✓	•	•
121910608.6	✓	✓	✓	✓	✓	•	✓
1016747	✓	✓	✓	✓	✓	✗	•
70731	✓	✓	✓	✓	✓	✗	✓
70782	✓	✓	✓	✓	✓	✗	✓
121612915	✓	✓	✓	✓	✓	•	✓
121614157	✓	✓	✓	✓	✓	✓	✓
1029093	✓	✓	✓	✓	✓	•	✓
1029122	✓	✓	✓	✓	✓	•	✓
1044999	✓	✓	✓	✓	✓	•	✓

APPENDIX: B

Title: Site Selection Criteria Checklist

Project	Geotechnical Site Investigation				
	Rock Strength	RQD	Rock Elevation	Rock Type	BH Map
1032593.01	✓	✓	✓	✓	✗
1056734	•	✓	✓	✓	✓
1017681	•	✓	✓	✓	✓
1020025	✓	✓	✓	✓	✗
1038917	✓	✓	✓	✓	✓
121612336	•	•	•	•	•
1021554	✗	✓	✓	✓	✓
52297	✗	•	•	•	✓
121612385	✓	✓	✓	✓	✓
1046136	✓	✓	✓	✓	✓
1049291	✓	✓	✓	✓	✓
1049353	✗	✓	✓	✓	✓
121613582	✓	✓	✓	✓	✓
121613585	✓	✓	✓	✓	✓
121611479	✓	✓	✓	✓	✓
7892J	✓	✓	✓	✓	✓
1031017	✗	✓	✓	✓	✓
121910608.6	✓	✓	✓	✓	✓
1016747	✓	✓	✓	✓	✓
70731	✗	•	•	•	✓
70782	✗	•	•	•	✓
121612915	✗	✓	✓	✓	✓
121614157	✓	✓	✓	✓	✓
1029093	✗	✗	✗	✗	✗
1029122	✗	✗	✗	✗	✗
1044999	✗	✗	✗	✗	✗

APPENDIX: B

Title: Site Selection Criteria Checklist

	Pile Type and Conditions		PDA Report				
Project	Pile Type/Size	In rock	Measured Toe	Toe Elevation	Pile Map	BOR	Blows/25 mm
1032730	✓	✓	✓	✓	✓	•	✓
1041042	✗	✗	✓	✓	✓	•	✓
121610496	✓	✓	✓	✓	✓	•	✓
121612305	✓	✓	✓	✓	✓	•	✓
6609	✓	✓	✓	✓	✓	•	✓
1038964	✗	✓	✓	✓	✓	•	✓
1040702	✓	✓	✓	✓	✓	•	✓
11562	✗	✓	✓	✓	✓	•	✓
11558	✓	✓	✓	✓	✓	•	✓
NSS52507	✗	✗	✓	✓	✓	•	✗
NSS52554	✓	✓	✓	✓	✓	•	✗
NSS52840	✓	✓	✓	✓	✓	•	✗
1024202	✓	✓	✓	✓	✓	•	✓
17604	✓	✗	✓	✓	✓	•	✓
14525	✓	✓	✓	✓	✓	•	✓
12162309	✓	✗	✓	✓	✓	•	✓
121612338	✓	✗	✓	✓	✓	•	✓
5649	✗	✓	✓	✓	✓	•	✓
1044801	✓	✓	✓	✓	✓	•	✓

APPENDIX: B

Title: Site Selection Criteria Checklist

	Geotechnical Site Investigation				
Project	Rock Strength	RQD	Rock Elevation	Rock Type	BH Map
1032730	✗	✗	✗	✗	✗
1041042	✓	✓	✗	✗	✓
121610496	✗	✗	✗	✗	✗
121612305	✗	✗	✗	✗	✗
6609	✗	✗	✗	✗	✗
1038964	✗	✗	✗	✗	✗
1040702	✗	✗	✗	✗	✗
11562	✗	✓	✗	✓	✓
11558	✗	✓	✗	✓	✓
NSS52507	✗	✓	✗	✗	✓
NSS52554	✗	✗	✗	✗	✗
NSS52840	✗	✓	✗	✓	✓
1024202	✗	✗	✗	✗	✗
17604	✗	✓	✗	✗	✓
14525	✗	✓	✗	✓	✓
12162309	✗	✓	✗	✗	✓
121612338	✓	✓	✗	✗	✓
5649	✗	✗	✗	✗	✗
1044801	✗	✗	✗	✓	✗

✓	Yes
•	Tested
•	Some
✗	No
	Project Data Used

Note:

-Some piles that didn't fit all criteria are not in this chart.

-There are multiple piles available on most sites.

APPENDIX C: LADANYI AND ROY (1971) ANALYSIS

APPENDIX: C

Title: Ladanyi and Roy (1971) as described in CFEM (2006), using B_1

Number	Measured (kN)	RQD	λ (discon/m)	Ksp	L/B
1056734	736	62	13.15	0.1	0.46
	850	62	13.15	0.1	0.00
1017681	1816	13	35.57	0.1	18.75
	1736	13	35.57	0.1	18.75
	1030	13	35.57	0.1	11.11
	950	13	35.57	0.1	11.11
121612385	2077	61	13.42	0.1	5.97
	3228	18	31.34	0.1	1.82
	1973	17	32.09	0.1	7.19
	2469	62	13.15	0.1	2.68
	3180	76	9.35	0.1	2.48
1046136	1472	66	12.07	0.1	0.00
	1205	64.5	12.47	0.1	7.10
121613582	894	41.1	19.82	0.1	19.53
	1041	1	66.38	0.1	15.81
121613585	791	17	32.09	0.1	1.68
121611479	915	1	66.38	0.1	6.29
	967	1	66.38	0.1	22.29
7892J	2057	79	8.53	0.1	0.00
	1976	92	5.00	0.1	0.00
121910608.6	762	70	10.98	0.1	11.94
1016746	631	10	12.98	0.1	18.20
121614157	1440	11	24.98	0.1	2.13

LEGEND

- High blows/25mm (not used)
- BOR (used)
- EOID (Not used)
- Same Pile EOID (Not used)

APPENDIX: C

Title: Ladanyi and Roy (1971) as described in CFEM (2006), using B_1

Number	Measured (kN)	L/t	d(L/B)	Calc B_1 (kN)	Calc Gross (kN)
1056734	736	15.79	1.19	26.70	234.52
	850	0.00	1.00	22.53	197.88
1017681	1816	480.77	3.00	280.26	1584.00
	1736	480.77	3.00	280.26	1584.00
	1030	256.41	3.00	152.10	1166.40
	950	256.41	3.00	152.10	1166.40
			1.00		
121612385	2077	120.11	3.00	314.28	2099.52
	3228	36.59	1.73	85.47	571.00
	1973	144.69	3.00	148.41	991.44
	2469	107.09	2.07	175.56	2292.64
	3180	99.21	1.99	168.89	2205.47
			1.00		
1046136	1472	0.00	1.00	33.75	230.64
	1205	141.99	3.00	101.26	691.92
121613582	894	392.74	3.00	279.36	1866.24
	1041	317.88	3.00	314.28	2099.52
121613585	791	33.77	1.67	38.17	260.14
121611479	915	126.62	3.00	125.63	856.25
	967	448.70	3.00	102.79	700.57
7892J	2057	0.00	1.00	50.10	288.30
	1976	0.00	1.00	143.79	827.42
121910608.6	762	336.36	3.00	96.75	929.77
	0				
121614157	1440	42.86	1.85	117.48	800.73

LEGEND

- High blows/25mm (not used)
- BOR (used)
- EOID (Not used)
- Same Pile EOID (Not used)

APPENDIX: C

Title: Ladanyi and Roy (1971) as described in CFEM (2006), using B_1

Measured	Calculated (Net)	Measured	Calculate (MPa)
736	27	78	3
1736	280	56	9
950	152	56	9
2077	314	107	16
1973	148	102	8
2469	176	125	9
3180	169	161	9
1205	101	86	7
894	279.36	46	14
791	38.17	56	3
915	125.63	65	9
967	102.79	69	7
2057	50.10	123	3
762	96.75	76	10
1440	117.48	102	8

Number	q_u (Mpa)	B_1 (m)	Spacing (m)	K_{sp}	d
1056734	8	0.324	0.033	0.1	1.19
1017681	10	0.40	0.028	0.1	3.00
	10	0.36	0.028	0.1	3.00
121612385	18	0.36	0.033	0.1	3.00
	8.5	0.36	0.031	0.1	3.00
	14.3	0.508	0.033	0.1	2.07
	14.3	0.508	0.033	0.1	1.99
1046136	8	0.31	0.033	0.1	3.00
121613582	16	0.36	0.050	0.1	3.00
121613585	5.4	0.31	0.031	0.1	1.67
121611479	9.9	0.31	0.048	0.1	3.00
	8.1	0.31	0.015	0.1	3.00
7892J	10	0.31	0.033	0.1	1.00
121910608.6	10.8	0.31	0.033	0.1	3.00
121614157	15	0.31	0.027	0.1	1.85

APPENDIX: C

Title: Ladanyi and Roy (1971): Predicted vs. Measured Regression Analysis, B_1

x	99.99%	-99.99%
0	0	0
10	164	12
20	329	24
30	493	35
40	658	47
50	822	59
60	986	71
70	1151	83
80	1315	94
90	1480	106
100	1644	118
110	1808	130
120	1973	142
130	2137	153
140	2302	165
150	2466	177
160	2630	189
170	2795	201

Base Area (m^2)	Measured (Mpa)	Calculate (kN)	Calculated (Mpa)
0.0094	78	27	2.8
0.0311	56	280	9.0
0.0169	56	152	9.0
0.0194	107	314	16.2
0.0194	102	148	7.7
0.0198	125	176	8.9
0.0198	161	169	8.5
0.0141	86	101	7.2
0.0194	46	279	14.4
0.0141	56	38	2.7
0.0141	65	126	8.9
0.0141	69	103	7.3
0.0167	123	50	3.0
0.0100	76	97	9.7
0.0141	102	117	8.3

APPENDIX: C

Title: Ladanyi and Roy (1971) as described in CFEM (2006), using B_2

Number	Measured (kN)	RQD	λ (discon/m)	c (m)	t (m)	δ/c (m)
1056734	736	62	13.15	0.076	0.010	0.005
	850	62	13.15	0.076	0.010	0.005
1017681	1816	13	35.57	0.028	0.016	0.005
	1736	13	35.57	0.028	0.016	0.005
	1030	13	35.57	0.028	0.016	0.005
	950	13	35.57	0.028	0.016	0.005
121612385	2077	61	13.42	0.074	0.018	0.005
	3228	18	31.34	0.032	0.018	0.005
	1973	17	32.09	0.031	0.018	0.005
	2469	62	13.15	0.076	0.013	0.005
	3180	76	9.35	0.107	0.013	0.005
1046136	1472	66	12.07	0.083	0.015	0.005
	1205	64.5	12.47	0.080	0.015	0.005
121613582	894	41.1	19.82	0.050	0.018	0.005
	1041	1	66.38	0.015	0.018	0.005
		0				
121613585	791	17	32.09	0.031	0.015	0.005
		0				
121611479	915	1	66.38	0.015	0.015	0.005
	967	1	67.38	0.015	0.015	0.005
		0				
7892J	2057	79	8.533	0.117	0.018	0.005
	1976	92	5	0.200	0.018	0.005
121910608.6	762	70	10.97826087	0.091	0.011	0.005
1016746	631	10	12.97826087	0.077	0.011	0.005
121614157	1440	11	24.97826087	0.040	0.015	0.005

LEGEND

High blows/25mm (not used)

BOR (used)

EOID (Not used)

Same Pile EOID (Not used)

APPENDIX: C

Title: Ladanyi and Roy (1971) as described in CFEM (2006), using B_2

Number	Measured (kN)	δ (m)	Ksp	L/t	d(L/t)	Calc B_2 (kN)
1056734	736	3.80E-04	0.95	15.79	3	642.10
	850	3.80E-04	0.95	0.00	1	214.03
1017681	1816	1.41E-04	0.41	480.77	3	1162.12
	1736	1.41E-04	0.41	480.77	3	1162.12
	1030	1.41E-04	0.41	256.41	3	630.70
	950	1.41E-04	0.41	256.41	3	630.70
121612385	2077	3.72E-04	0.62	120.11	3	1943.48
	3228	1.60E-04	0.41	36.59	3	612.87
	1973	1.56E-04	0.41	144.69	3	607.52
	2469	3.80E-04	0.78	107.09	3	1973.59
	3180	5.35E-04	0.99	99.21	3	2508.67
1046136	1472	4.14E-04	0.72	0.00	1	243.35
	1205	4.01E-04	0.71	141.99	3	714.77
121613582	894	2.52E-04	0.50	392.74	3	1403.70
	1041	7.53E-05	0.33	317.88	3	1042.49
121613585	791	1.56E-04	0.43	33.77	3	297.24
121611479	915	7.53E-05	0.34	126.62	3	431.55
	967	7.42E-05	0.34	448.70	3	351.80
7892J	2057	5.86E-04	0.81	0.00	1	406.83
	1976	1.00E-03	1.20	0.00	1	1729.37
121910608.6	762	4.55E-04	0.97	336.36	3	942.41
1016746	631	3.85E-04	0.89	429.25	3	1596.07
121614157	1440	2.00E-04	0.48	42.86	3	920.37

LEGEND

High blows/25mm (not used)

BOR (used)

EOID (Not used)

Same Pile EOID (Not used)

APPENDIX: C

Title: Ladanyi and Roy (1971) as described in CFEM (2006), using B_2

Measured (kN)	Calculated (kN)	ase Area (m	Measured (MPa)	Calculated (MPa)
736	642.10	0.009	78.4	68.4
1736	1162.12	0.031	55.7	37.3
950	630.70	0.017	56.2	37.3
2077	1943.48	0.019	107.1	100.2
1973	607.52	0.019	101.7	31.3
2469	1973.59	0.020	124.9	99.9
3180	2508.67	0.020	160.9	126.9
1205	714.77	0.014	85.7	50.8
894	1403.70	0.019	46.1	72.4
791	297.24	0.014	56.1	21.1
915	431.55	0.014	64.9	30.6
967	351.80	0.014	68.6	25.0
2057	406.83	0.017	123.2	24.4
762	942.41	0.010	76.2	94.2
1440	920.37	0.014	102.1	65.3

Measured (kN)	Calculated (kN)	ase Area (m	Measured (MPa)	Calculated (MPa)
850	214	0.0094	90.6	22.8
3228	613	0.0194	166.4	31.6
1472	243	0.0141	104.7	17.3
1041	1042	0.0194	53.7	53.7
1976	1729	0.0167	118.3	103.6
631	1596	0.0080	78.9	199.5

x	99.99%	-99.99%
0	0	0
10	21	5
20	41	9
30	62	14
40	82	19
50	103	24
60	123	28
70	144	33
80	164	38
90	185	42
100	205	47
110	226	52
120	246	56
130	267	61
140	287	66
150	308	71

APPENDIX: C

Title: Best Fit Predicted vs. Measured Regression Analysis

Measured (kN)	Calculated (kN)	Base Area (m^2)	Measured (MPa)	Calculated (MPa)
736	563.18	0.009	78.4	60.0
1736	2335.50	0.031	55.7	75.0
950	1267.50	0.017	56.2	75.0
2077	2619.00	0.019	107.1	135.0
1973	1236.75	0.019	101.7	63.8
2469	2119.43	0.020	124.9	107.3
3180	2119.43	0.020	160.9	107.3
1205	843.87	0.014	85.7	60.0
894	2328.00	0.019	46.1	120.0
791	571.05	0.014	56.1	40.5
915	1046.93	0.014	64.9	74.3
967	856.58	0.014	68.6	60.8
2057	1252.50	0.017	123.2	75.0
762	806.25	0.010	76.2	80.6
1440	1586.25	0.014	102.1	112.5

Measured (kN)	Calculated (kN)	Base Area (m^2)	Measured (MPa)	Calculated (MPa)
850	563	0.0094	90.6	60.0
3228	1237	0.0194	166.4	63.8
1472	844	0.0141	104.7	60.0
1041	2619	0.0194	53.7	135.0
1976	3595	0.0167	118.3	215.3
631	1500	0.0080	78.9	187.5

Calc	-99.99%	99.99%
0	0	0
500	235	763
1000	470	1526
1500	704	2288
2000	939	3051
2500	1174	3814

Interval (%)	Lower Bound	Upper Bound
95	0.79	1.21
98	0.74	1.26
99.9	0.59	1.41
99.99	0.47	1.53